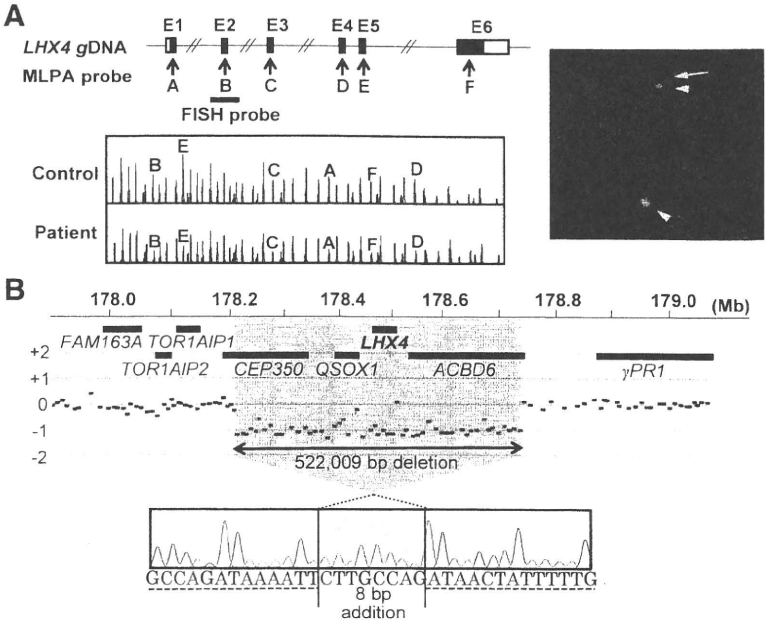

FIG. 1. Gene copy number analysis. Panel A, MLPA and FISH analyses. The *black and white boxes* on genomic DNA (gDNA) denote the coding regions on exons 1–6 (E1–E6) and the untranslated regions, respectively. The sites examined by MLPA probes (A–F) are indicated by *arrows*, and the region identified by the 5305-bp FISH probe is shown by a *thick horizontal line*. In MLPA analysis, the peaks for the sites A–F are reduced in the patient. The *red* peaks indicate the internal size markers. In FISH analysis, the *red* signal is derived from the probe for *LHX4*, and the *green* signals are derived from chromosome 1 centromere control probe (Cytocell, Cambridge, UK) used as an internal control. The probe for *LHX4* is labeled with digoxigenin and detected by rhodamine antidigoxigenin, and the control probe is labeled with biotin and detected by avidin conjugated to fluorescein isothiocyanate. Panel B, Oligoarray CGH analysis and direct sequencing of the deletion junction. The deletion is 522,009 bp in physical size (*shaded in gray*) and is associated with an addition of an 8-bp segment of unknown origin (*highlighted in yellow*). The normal sequences flanking the microdeletion are indicated with *dashed underlines*.

parental samples revealed *LHX3*-p.T63M and *LHX3*-p.A322T in the phenotypically normal mother and father, respectively; parental analysis was refused for *LHX4*-p.V201I, *LHX4*-p.H387P, and *SOX3*-p.V53L. Thus, four missense variants except for *LHX4*-p.V201I were found in healthy controls or parents. For *LHX4*-p.V201I, functional studies showed a normal transactivation function for the *POU1F1* promoter, with no dominant-negative effect (Supplemental Fig. 1). *In silico* analyses indicated that the V201 and the H387 residues in *LHX4* and the A322 residue in *LHX3* were well conserved, whereas the T63 in *LHX3* and the V53 in *SOX3* were poorly conserved (Supplemental Table 2). Furthermore, it was predicted that *LHX4*-V201I and *LHX4*-H387P were unlikely to influence ESEs, whereas *LHX3*-T63M and *LHX3*-A322T might affect ESEs (Supplemental Table 3). None of the missense variants were predicted to influence splice sites (Supplemental Table 4).

Identification of a microdeletion involving *LHX4*

A heterozygous deletion involving *LHX4* was indicated by MLPA and confirmed by FISH (Fig. 1A). Oligoarray CGH and sequencing of the fusion point showed that the deletion was 522,009 bp in physical size and was associated with an addition of an 8-bp segment of unknown origin (Fig. 1B). There were no repeat sequences around the deletion breakpoints. The deletion also affected *CEP350*, *QSOX1*, and *ACBD6*. This microdeletion was absent from the parents.

Patient with the microdeletion

This Japanese female patient was born at 40 wk gestation after an uncomplicated pregnancy and delivery. At birth, her length was 48.0 cm (−0.2 SD), her weight 2.59 kg (−1.0 SD), and her head circumference 33 cm (−0.1 SD). She had transient respiratory distress and hypoglycemia in the early neonatal period. Furthermore, biochemical studies for prolonged jaundice indicated central hypothyroidism at 1 month of age (Table 1). Thus, she was placed on thyroid hormone replacement therapy.

At 1 yr 6 months of age, she was referred to us because of severe short stature. Her height was 64.5 cm (−5.1 SD), and her weight was 6.2 kg (−2.8 SD). Endocrine studies at that time revealed severe GH and prolactin deficiencies (Table 1). Her karyotype was 46,XX in all 50 lymphocytes examined. Recombinant human GH therapy (0.175 mg/kg·wk) was started at 1 yr 8 months of age, showing a remarkable effect. Brain magnetic resonance imaging at 5 yr of age delineated anterior pituitary hypoplasia with a small cystic lesion, ectopic posterior pituitary, and underdeveloped sella turcica (Supplemental Fig. 2). At 11 yr of age, a GnRH test was performed due to lack of pubertal signs, revealing gonadotropin deficiencies (Table 1). Thus, sex steroid replacement therapy was started at 13 yr of age. She had no episode of adrenal insufficiency, with normal blood ACTH and cortisol values at yearly examinations. A CRH stimulation test at 17 yr of age also showed an apparently normal hypothalamic-pituitary-adrenal (HPA) function (Table 1). On the last examination at 17 yr old, she measured 148.7 cm (−1.8 SD), weighed 45.6 kg (−0.9 SD), and manifested full pubertal development. She had no developmental retardation.

The nonconsanguineous parents and the three brothers were clinically normal. The father was 164 cm (−1.2 SD) tall, and the mother was 155 cm (−0.6 SD) tall.

TABLE 1. Blood hormone values of the patient with *LHX4* deletion

			1.5 yr		11 yr		17 yr	
	Stimulus (dosage)	**1 month, basal**	**Basal**	**Peak**	**Basal**	**Peak**	**Basal**	**Peak**
GH (ng/ml)	GHRH (1 mg/kg)		0.2	**1.2**				
	Arginine (0.5 g/kg)		0.1	**0.2**				
	L-Dopa (10 mg/kg)		0.1	**0.1**				
LH (mIU/ml)	GnRH (100 mg/m^2)		<0.5		0.3	**0.8**		
FSH (mIU/ml)	GnRH (100 mg/m^2)		0.5		1.3	**1.6**		
TSH (mU/ml)	TRH (10 mg/kg)	3.5	2.3[a]	**3.9**[a]				
Prolactin (ng/ml)	TRH (10 mg/kg)		**<1.0**	**<1.0**				
ACTH (pg/ml)[b]	CRH (2 mg/kg)		24.6		26.4		26.1	118.7
Cortisol (μg/dl)[b]	CRH (2 mg/kg)		17.5		10.6		15.7	37.82
IGF-I (ng/ml)			**9**					
Free T_4 (ng/dl)		**0.6**	**1.1**[a]					
Estradiol (pg/ml)					**<15**			

The conversion factors to the SI unit are as follows: GH 1.0 (μg/liter), LH 1.0 (IU/liter), FSH 1.0 (IU/liter), TSH 1.0 (mIU/liter), prolactin 1.0 (μg/liter), ACTH 0.22 (pmol/liter), cortisol 27.59 (nmol/liter), IGF-I 0.131 (nmol/liter), free T_4 12.87 (pmol/liter), and estradiol 3.671 (pmol/liter). Hormone values have been evaluated by the age- and sex-matched Japanese reference data; low hormone data are in *bold*. Blood sampling during the provocation tests were done at 0, 30, 60, 90, and 120 min.

[a] Examined under T_4 supplementation therapy.

[b] Obtained at 0800 h.

Discussion

We performed sequence and gene copy number analyses for all coding exons of six previously known genes in 71 patients with CPHD, although noncoding regions were not examined. Consequently, we could identify only a single patient with a heterozygous microdeletion involving *LHX4*. This indicates the rarity of abnormalities affecting the six genes in patients with CPHD and, at the same time, the significance of the gene copy number analysis in such patients. In this regard, because gene copy number aberrations have been found for multiple genes including microdeletions of *PROP1* and *LHX3* and microduplications of *SOX3* (7–9, 14, 15), this implies that gene copy number aberrations should be screened in genetic diagnosis.

Several matters are noteworthy for the clinical and molecular findings of the patient with the microdeletion involving *LHX4*. First, the HPA function was preserved normally at 17 yr of age. However, ACTH deficiency has often been identified in the previously reported patients with heterozygous intragenic loss-of-function mutations of *LHX4* (Supplemental Table 5), and the HPA function often deteriorates with age in patients with CPHD (2). Thus, careful follow-up is necessary for the HPA function of this patient. Second, the microdeletion has affected three additional genes. In this context, the pituitary phenotype of this patient remains within the clinical spectrum of patients with *LHX4* mutations (Supplemental Table 5), and there was no discernible extrapituitary phenotype. Thus, hemizygosity for the three genes would not have a major clinical effect, if any. Third, the deletion breakpoints resided on nonrepeat sequences, and the fusion point was associated with an addition of an 8-bp segment of unknown origin. This indicates that the deletion has been produced by nonhomologous end joining, *i.e.* an aberrant breakage and re-union between nonhomologous sequences (16).

We also identified five novel heterozygous missense substitutions. In this regard, the data obtained from sequencing analysis in control subjects and available parents, functional studies, and *in silico* analyses argue against the five missense substitutions being a disease-causing pathological mutation, although the possibility that they might function as a susceptibility factor for the development of CPHD remains tenable. In particular, *LHX4*-p.V201I, which was absent from 100 control subjects and affected the well-conserved V201 residue, may have been erroneously regarded as a pathological mutation, unless additional studies were performed. Indeed, *LHX4*-p.V201I exerted no predictable effect on the splicing pattern and had a normal transactivation activity in the used system, although transactivation function may be variable depending on the used promoters and cells (17). Such rare variants with an apparently normal function have also been reported previously (3, 18). Thus, whereas *in vitro* experimental data and *in silico* prediction data may not precisely reflect *in vivo* functions, it is recommended to perform such studies for novel substitutions, especially missense substitutions.

In summary, the results imply the rarity of pathological abnormalities in the previously known genes in patients with CPHD and the significance of the gene copy number analysis in such patients. Thus, the causes of CPHD remain elusive in most patients, and additional studies are required to clarify the underlying factors for the development of CPHD.

Acknowledgments

We thank the patients and the parents for participating in this study. We also thank Dr. Takizawa and Dr. Morita for participating in medical care of the reported patients.

Address all correspondence and requests for reprints to: Dr. T. Ogata, Department of Endocrinology and Metabolism, National Research Institute for Child Health and Development, 2-10-1 Ohkura, Setagaya, Tokyo 157-8535, Japan. E-mail: tomogata@nch.go.jp.

This work was supported by Grants for Child Health and Development (20C-2) and Research on Children and Families (H21-005) from the Ministry of Health, Labor, and Welfare and by Grants-in-Aid for Young Scientists (B) (21791025) from the Ministry of Education, Culture, Sports, Science, and Technology, Japan.

Disclosure Summary: All authors report no conflicts of interest.

References

1. **Cohen LE, Radovick S** 2002 Molecular basis of combined pituitary hormone deficiencies. Endocr Rev 23:431–442
2. **Kelberman D, Rizzoti K, Lovell-Badge R, Robinson IC, Dattani MT** 2009 Genetic regulation of pituitary gland development in human and mouse. Endocr Rev 30:790–829
3. **Dateki S, Kosaka K, Hasegawa K, Tanaka H, Azuma N, Yokoya S, Muroya K, Adachi M, Tajima T, Motomura K, Kinoshita E, Moriuchi H, Sato N, Fukami M, Ogata T** 2010 Heterozygous orthodenticle homeobox 2 mutations are associated with variable pituitary phenotype. J Clin Endocrinol Metab 95:756–764
4. **Coya R, Vela A, Pérez de Nanclares G, Rica I, Castaño L, Busturia MA, Martul P; GEDPIT group** 2007 Panhypopituitarism: genetic versus acquired etiological factors. J Pediatr Endocrinol Metab 20: 27–36
5. **Mehta A, Hindmarsh PC, Mehta H, Turton JP, Russell-Eggitt I, Taylor D, Chong WK, Dattani MT** 2009 Congenital hypopituitarism: clinical, molecular and neuroradiological correlates. Clin Endocrinol (Oxf) 71:376–382
6. **Reynaud R, Gueydan M, Saveanu A, Vallette-Kasic S, Enjalbert A, Brue T, Barlier A** 2006 Genetic screening of combined pituitary hormone deficiency: experience in 195 patients. J Clin Endocrinol Metab 91:3329–3336
7. **Abrão MG, Leite MV, Carvalho LR, Billerbeck AE, Nishi MY, Barbosa AS, Martin RM, Arnhold IJ, Mendonca BB** 2006 Combined pituitary hormone deficiency (CPHD) due to a complete PROP1 deletion. Clin Endocrinol (Oxf) 65:294–300
8. **Pfaeffle RW, Savage JJ, Hunter CS, Palme C, Ahlmann M, Kumar P, Bellone J, Schoenau E, Korsch E, Brämswig JH, Stobbe HM, Blum WF, Rhodes SJ** 2007 Four novel mutations of the *LHX3* gene cause combined pituitary hormone deficiencies with or without limited neck rotation. J Clin Endocrinol Metab 92:1909–1919
9. **Woods KS, Cundall M, Turton J, Rizotti K, Mehta A, Palmer R, Wong J, Chong WK, Al-Zyoud M, El-Ali M, Otonkoski T, Martinez-Barbera JP, Thomas PQ, Robinson IC, Lovell-Badge R, Woodward KJ, Dattani MT** 2005 Over- and underdosage of SOX3 is associated with infundibular hypoplasia and hypopituitarism. Am J Hum Genet 76:833–849
10. **Machinis K, Amselem S** 2005 Functional relationship between *LHX4* and *POU1F1* in light of the *LHX4* mutation identified in patients with pituitary defects. J Clin Endocrinol Metab 90:5456–5462
11. **Cartegni L, Chew SL, Krainer AR** 2002 Listening to silence and understanding nonsense: exonic mutations that affect splicing. Nat Rev Genet 3:285–298
12. **Strachan T, Read AP** 2004 Instability of the human genome: mutation and DNA repair. In: Human molecular genetics. 3rd ed. London and New York: Garland Science; 334–337
13. **Schouten JP, McElgunn CJ, Waaijer R, Zwijnenburg D, Diepvens F, Pals G** 2002 Relative quantification of 40 nucleic acid sequences by multiplex ligation-dependent probe amplification. Nucleic Acids Res 30:e57
14. **Desviat LR, Pérez B, Ugarte M** 2006 Identification of exonic deletions in the PAH gene causing phenylketonuria by MLPA analysis. Clin Chim Acta 373:164–167
15. **Fukami M, Dateki S, Kato F, Hasegawa Y, Mochizuki H, Horikawa R, Ogata T** 2008 Identification and characterization of cryptic *SHOX* intragenic deletions in three Japanese patients with Léri-Weill dyschondrosteosis. J Hum Genet 53:454–459
16. **Shaw CJ, Lupski JR** 2004 Implications of human genome architecture for rearrangement-based disorders: the genomic basis of disease. Hum Mol Genet 13:R57–R64
17. **Ito M, Achermann JC, Jameson JL** 2000 A naturally occurring steroidogenic factor-1 mutation exhibits differential binding and activation of target genes. J Biol Chem 275:31708–31714
18. **Castinetti F, Saveanu A, Reynaud R, Quentien MH, Buffin A, Brauner R, Kaffel N, Albarel F, Guedj AM, El Kholy M, Amin M, Enjalbert A, Barlier A, Brue T** 2008 A novel dysfunctional *LHX4* mutation with high phenotypical variability in patients with hypopituitarism. J Clin Endocrinol Metab 93:2790–2799

The IG-DMR and the *MEG3*-DMR at Human Chromosome 14q32.2: Hierarchical Interaction and Distinct Functional Properties as Imprinting Control Centers

Masayo Kagami[1], Maureen J. O'Sullivan[2], Andrew J. Green[3,4], Yoshiyuki Watabe[5], Osamu Arisaka[5], Nobuhide Masawa[6], Kentarou Matsuoka[7], Maki Fukami[1], Keiko Matsubara[1], Fumiko Kato[1], Anne C. Ferguson-Smith[8], Tsutomu Ogata[1]*

1 Department of Endocrinology and Metabolism, National Research Institute for Child Health and Development, Tokyo, Japan, **2** Department of Pathology, School of Medicine, Our Lady's Children's Hospital, Trinity College, Dublin, Ireland, **3** National Center for Medical Genetics, University College Dublin, Our Lady's Hospital, Dublin, Ireland, **4** School of Medicine and Medical Science, University College, Dublin, Ireland, **5** Department of Pediatrics, Dokkyo University School of Medicine, Tochigi, Japan, **6** Department of Pathology, Dokkyo University School of Medicine, Tochigi, Japan, **7** Department of Pathology, National Center for Child Health and Development, Tokyo, Japan, **8** Department of Physiology, Development and Neuroscience, University of Cambridge, Cambridge, United Kingdom

Abstract

Human chromosome 14q32.2 harbors the germline-derived primary *DLK1-MEG3* intergenic differentially methylated region (IG-DMR) and the postfertilization-derived secondary *MEG3*-DMR, together with multiple imprinted genes. Although previous studies in cases with microdeletions and epimutations affecting both DMRs and paternal/maternal uniparental disomy 14-like phenotypes argue for a critical regulatory function of the two DMRs for the 14q32.2 imprinted region, the precise role of the individual DMR remains to be clarified. We studied an infant with upd(14)pat body and placental phenotypes and a heterozygous microdeletion involving the IG-DMR alone (patient 1) and a neonate with upd(14)pat body, but no placental phenotype and a heterozygous microdeletion involving the *MEG3*-DMR alone (patient 2). The results generated from the analysis of these two patients imply that the IG-DMR and the *MEG3*-DMR function as imprinting control centers in the placenta and the body, respectively, with a hierarchical interaction for the methylation pattern in the body governed by the IG-DMR. To our knowledge, this is the first study demonstrating an essential long-range imprinting regulatory function for the secondary DMR.

Citation: Kagami M, O'Sullivan MJ, Green AJ, Watabe Y, Arisaka O, et al. (2010) The IG-DMR and the *MEG3*-DMR at Human Chromosome 14q32.2: Hierarchical Interaction and Distinct Functional Properties as Imprinting Control Centers. PLoS Genet 6(6): e1000992. doi:10.1371/journal.pgen.1000992

Editor: Wolf Reik, The Babraham Institute, United Kingdom

Received December 29, 2009; **Accepted** May 19, 2010; **Published** June 17, 2010

Funding: This work was supported by grants from the Ministry of Health, Labor, and Welfare; from the Ministry of Education, Science, Sports and Culture; and from Takeda Science Foundation. The funders had no role in study design, data collection and analysis, decision to publish, or preparation of the manuscript.

Competing Interests: The authors have declared that no competing interests exist.

* E-mail: tomogata@nch.go.jp

Introduction

Human chromosome 14q32.2 carries a cluster of protein-coding paternally expressed genes (*PEGs*) such as *DLK1* and *RTL1* and non-coding maternally expressed genes (*MEGs*) such as *MEG3* (alias, *GTL2*), *RTL1as* (*RTL1* antisense), *MEG8*, *snoRNAs*, and *microRNAs* [1,2]. Consistent with this, paternal uniparental disomy 14 (upd(14)pat) results in a unique phenotype characterized by facial abnormality, small bell-shaped thorax, abdominal wall defects, placentomegaly, and polyhydramnios [2,3], and maternal uniparental disomy 14 (upd(14)mat) leads to less-characteristic but clinically discernible features including growth failure [2,4].

The 14q32.2 imprinted region also harbors two differentially methylated regions (DMRs), i.e., the germline-derived primary *DLK1-MEG3* intergenic DMR (IG-DMR) and the postfertilization-derived secondary *MEG3*-DMR [1,2]. Both DMRs are hypermethylated after paternal transmission and hypomethylated after maternal transmission in the body, whereas in the placenta the IG-DMR alone remains as a DMR and the *MEG3*-DMR is rather hypomethylated [1,2]. Furthermore, previous studies in cases with upd(14)pat/mat-like phenotypes have revealed that epimutations (hypermethylation) and microdeletions affecting both DMRs of maternal origin cause paternalization of the 14q32.2 imprinted region, and that epimutations (hypomethylation) affecting both DMRs of paternal origin cause maternalization of the 14q32.2 imprinted region, while microdeletions involving the DMRs of paternal origin have no effect on the imprinting status [2,5–8]. These findings, together with the notion that parent-of-origin specific expression patterns of imprinted genes are primarily dependent on the methylation status of the DMRs [9], argue for a critical regulatory function of the two DMRs for the 14q32.2 imprinted region, with possible different effects between the body and the placenta.

However, the precise role of individual DMR remains to be clarified. Here, we report that the IG-DMR and the *MEG3*-DMR show a hierarchical interaction for the methylation pattern in the body, and function as imprinting control centers in the placenta and the body, respectively. To our knowledge, this is the first study demonstrating not only different roles between the primary and secondary DMRs at a single imprinted region, but also an essential regulatory function for the secondary DMR.

Author Summary

Genomic imprinting is a process causing genes to be expressed in a parent-of-origin specific manner—some imprinted genes are expressed from maternally inherited chromosomes and others from paternally inherited chromosomes. Imprinted genes are often located in clusters regulated by regions that are differentially methylated according to their parental origin. The human chromosome 14q32.2 imprinted region harbors the germline-derived primary *DLK1-MEG3* intergenic differentially methylated region (IG-DMR) and the postfertilization-derived secondary *MEG3*-DMR, together with multiple imprinted genes. Perturbed dosage of these imprinted genes, for example in patients with paternal and maternal uniparental disomy 14, causes distinct phenotypes. Here, through analysis of patients with microdeletions recapitulating some or all of the uniparental disomy 14 phenotypes, we show that the IG-DMR acts as an upstream regulator for the methylation pattern of the *MEG3*-DMR in the body but not in the placenta. Importantly, in the body, the *MEG3*-DMR functions as an imprinting control center. To our knowledge, this is the first study demonstrating an essential function for the secondary DMR in the regulation of multiple imprinted genes. Thus, the results provide a significant advance in the clarification of underlying epigenetic features that can act to regulate imprinting.

Results

Clinical reports

We studied an infant with upd(14)pat body and placental phenotypes (patient 1) and a neonate with upd(14)pat body, but no placental, phenotype (patient 2) (Figure 1). Detailed clinical features of patients 1 and 2 are shown in Table 1. In brief, patient 1 was delivered by a caesarean section at 33 weeks of gestation due to progressive polyhydramnios despite amnioreduction at 28 and 30 weeks of gestation, whereas patient 2 was born at 28 weeks of gestation by a vaginal delivery due to progressive labor without discernible polyhydramnios. Placentomegaly was observed in patient 1 but not in patient 2. Patients 1 and 2 were found to have characteristic face, small bell-shaped thorax with coat hanger appearance of the ribs, and omphalocele. Patient 1 received surgical treatment for omphalocele immediately after birth and mechanical ventilation for several months. At present, she is 5.5 months of age, and still requires intensive care including oxygen administration and tube feeding. Patient 2 died at four days of age due to massive intracranial hemorrhage, while receiving intensive care including mechanical ventilation. The mother of patient 1 had several non-specific clinical features such as short stature and obesity. The father of patient 1 and the parents of patient 2 were clinically normal.

Sample preparation

We isolated genomic DNA (gDNA) and transcripts (*mRNAs*, *snoRNAs*, and *microRNAs*) from fresh leukocytes of patients 1 and the parents of patients 1 and 2, from fresh skin fibroblasts of patient 2, and from formalin-fixed and paraffin-embedded placental samples of patient 1 and similarly treated pituitary and adrenal samples of patient 2 (although multiple body tissues were available in patient 2, useful gDNA and transcript samples were not obtained from other tissues probably due to drastic post-mortem degradation). We also made metaphase spreads from leukocytes and skin fibroblasts. For comparison, we obtained control samples from fresh normal adult leukocytes, neonatal skin fibroblasts, and placenta at 38 weeks of gestation, and from fresh leukocytes of upd(14)pat/mat patients and formalin-fixed and paraffin-embedded placenta of a upd(14)pat patient [2,3].

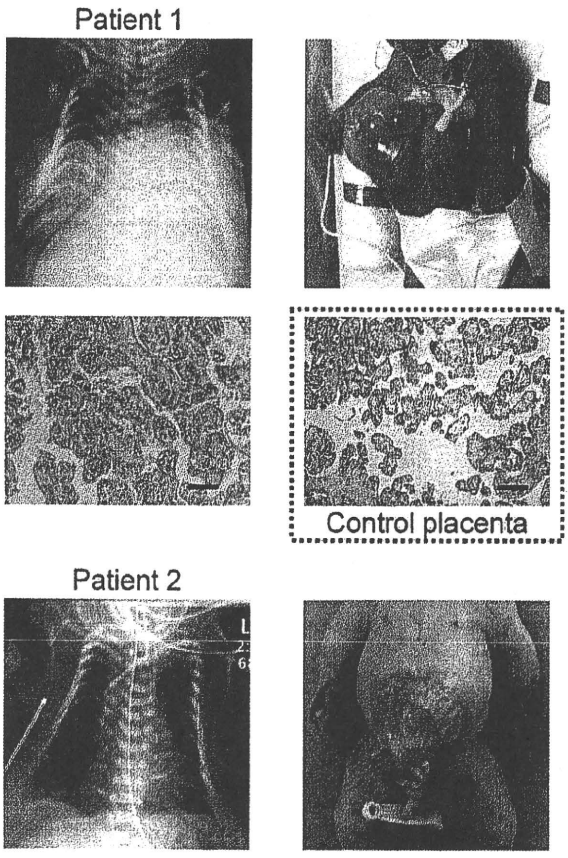

Figure 1. Clinical phenotypes of patients 1 and 2 at birth. Both patients have bell shaped thorax with coat hanger appearance of the ribs and omphalocele. In patient 1, histological examination of the placenta shows proliferation of dilated and congested chorionic villi, as has previously been observed in a case with upd(14)pat [2]. For comparison, the histological finding of a gestational age matched (33 weeks) control placenta is shown in a dashed square. The horizontal black bars indicate 100 μm.
doi:10.1371/journal.pgen.1000992.g001

Structural analysis of the imprinted region

We first examined the structure of the 14q32.2 imprinted region (Figure 2). Upd(14) was excluded in patients 1 and 2 as well as in the mother of patient 1 by microsatellite analysis (Table S1), and FISH analysis for the two DMRs identified a familial heterozygous deletion encompassing the IG-DMR alone in patient 1 and her mother and a *de novo* heterozygous deletion encompassing the *MEG3*-DMR alone in patient 2 (Figure 2). The microdeletions were further localized by SNP genotyping for 70 loci (Table S1) and quantitative real-time PCR (q-PCR) analysis for four regions around the DMRs (Figure S1A), and serial direct sequencing for the long PCR products harboring the deletion junctions successfully identified the fusion points of the microdeletions in patient 1 and her mother and in patient 2 (Figure 2). According to the NT_026437 sequence data at the NCBI Database (Genome Build 36.3) (http://preview.ncbi.nlm.nih.gov/guide/), the deletion

Table 1. Clinical features in patients 1 and 2.

	Patient 1	Patient 2	Upd(14)pat (n = 20)[c]
Present age	5.5 months	Deceased at 4 days	0–9 years
Sex	Female	Female	Male:Female = 9:11
Karyotype	46,XX	46,XX	
Pregnancy and delivery			
Gestational age (weeks)	33	28	28–37
Delivery	Caesarean	Vaginal	Vaginal:Caesarean = 6:7
Polyhydramnios	Yes	No	20/20 (<28)[d]
Amnioreduction (weeks)	2× (28, 30)	No	6/6
Placentomegaly	Yes	No	10/10
Growth pattern			
Prenatal growth failure	No	No	1/13
Birth length (cm)	43 (WNR)[a]	34 (WNR)[a]	
Birth weight (kg)	2.84 (>90 centile)[a]	1.32 (WNR)[a]	
Postnatal growth failure	Yes	…	5/6
Present stature (cm)	56.3 (−3.0 SD)[b]	…	
Present weight (kg)	5.02 (−3.0 SD)[b]	…	
Characteristic face			
Frontal bossing	No	Yes	5/7
Hairy forehead	Yes	Yes	9/10
Blepharophimosis	Yes	No	14/15
Depressed nasal bridge	Yes	Yes	13/13
Anteverted nares	Yes	No	6/10
Small ears	Yes	Yes	11/12
Protruding philtrum	Yes	No	15/15
Puckered lips	No	No	3/10
Micrognathia	Yes	Yes	11/12
Thoracic abnormality			
Bell-shaped thorax	Yes	Yes	17/17
Mechanical ventilation	Yes	Yes	17/17
Abdominal wall defect			
Diastasis recti	…	…	15/17
Omphalocele	Yes	Yes	2/17[e]
Others			
Short webbed neck	Yes	Yes	14/14
Cardiac disease	No	Yes (PDA)	5/10
Inguinal hernia	No	No	2/6
Coxa valga	Yes	No	3/4
Joint contractures	Yes	No	8/10
Kyphoscoliosis	No	No	4/7
Extra features		Hydronephrosis (bilateral)	

WNR: within the normal range; SD: standard deviation; and PDA: patent ductus arteriosus.

a Assessed by the gestational age- and sex-matched Japanese reference data from the Ministry of Health, Labor, and Welfare (http://www.e-stat.go.jp/SG1/estat/GL02020101.do).

b Assessed by the age- and sex-matched Japanese reference data..

c In the column summarizing the clinical features of 20 patients with upd(14)pat, the denominators indicate the number of cases examined for the presence or absence of each feature, and the numerators represent the number of cases assessed to be positive for that feature; thus, the differences between the denominators and the numerators denote the number of cases evaluated to be negative for that feature (adopted from reference [2]).

d Polyhydramnios has been identified by 28 weeks of gestation.

e Omphalocele is present in two cases with upd(14)pat and in two cases with epimutations [2].

doi:10.1371/journal.pgen.1000992.t001

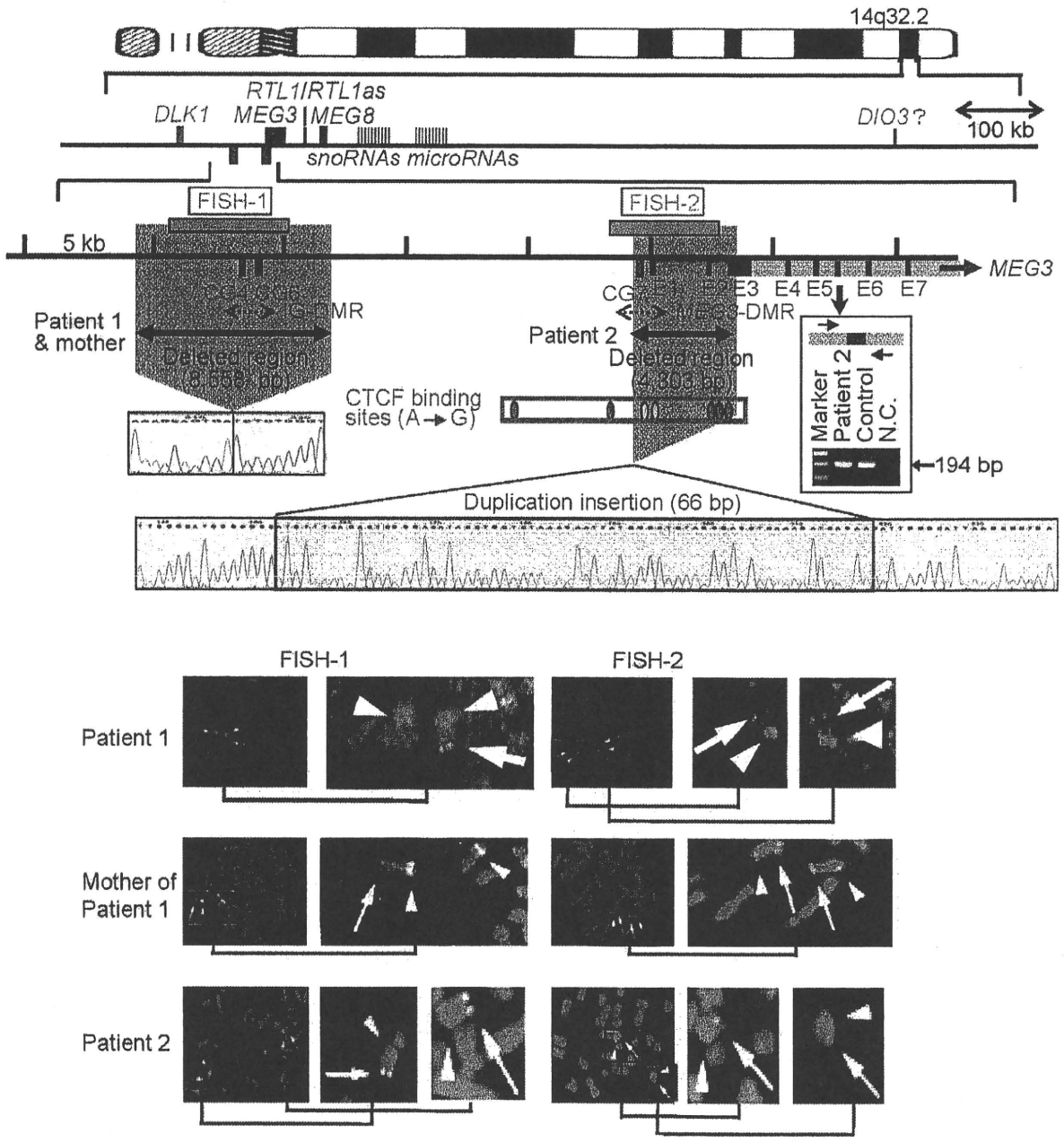

Figure 2. Physical map of the 14q32.2 imprinted region and the deleted segments in patient 1 and her mother and in patient 2 (shaded in gray). *PEGs* are shown in blue, *MEGs* in red, and the IG-DMR (CG4 and CG6) and the *MEG3*-DMR (CG7) in green. It remains to be clarified whether *DIO3* is a *PEG*, although mouse *Dio3* is known to be preferentially but not exclusively expressed from a paternally derived chromosome [35]. For *MEG3*, the isoform 2 with nine exons (red bars) and eight introns (light red segment) is shown (Ensembl; http://www.ensembl.org/index.html). Electrochromatograms represent the fusion point in patient 1 and her mother, and the fusion point accompanied by insertion of a 66 bp segment (highlighted in blue) with a sequence identical to that within *MEG3* intron 5 (the blue bar) in patient 2. Since PCR amplification with primers flanking the 66 bp segment at *MEG3* intron 5 has produced a 194 bp single band in patient 2 as well as in a control subject (shown in the box), this indicates that the 66 bp segment at the fusion point is caused by a duplicated insertion rather than by a transfer from intron 5 to the fusion point (if the 66 bp is transferred from the original position, a 128 bp band as well as a 194 bp band should be present in patient 2) (the marker size: 100, 200, and 300 bp). In the FISH images, the red signals (arrows) have been identified by the FISH-1 probe and the FISH-2 probe, and the light green signals (arrowheads) by the RP11-566I2 probe for 14q12 used as an internal control. The faint signal detected by the FISH-2 probe in patient 2 is consistent with the preservation of a ~1.2 kb region identified by the centromeric portion of the FISH-2 probe.
doi:10.1371/journal.pgen.1000992.g002

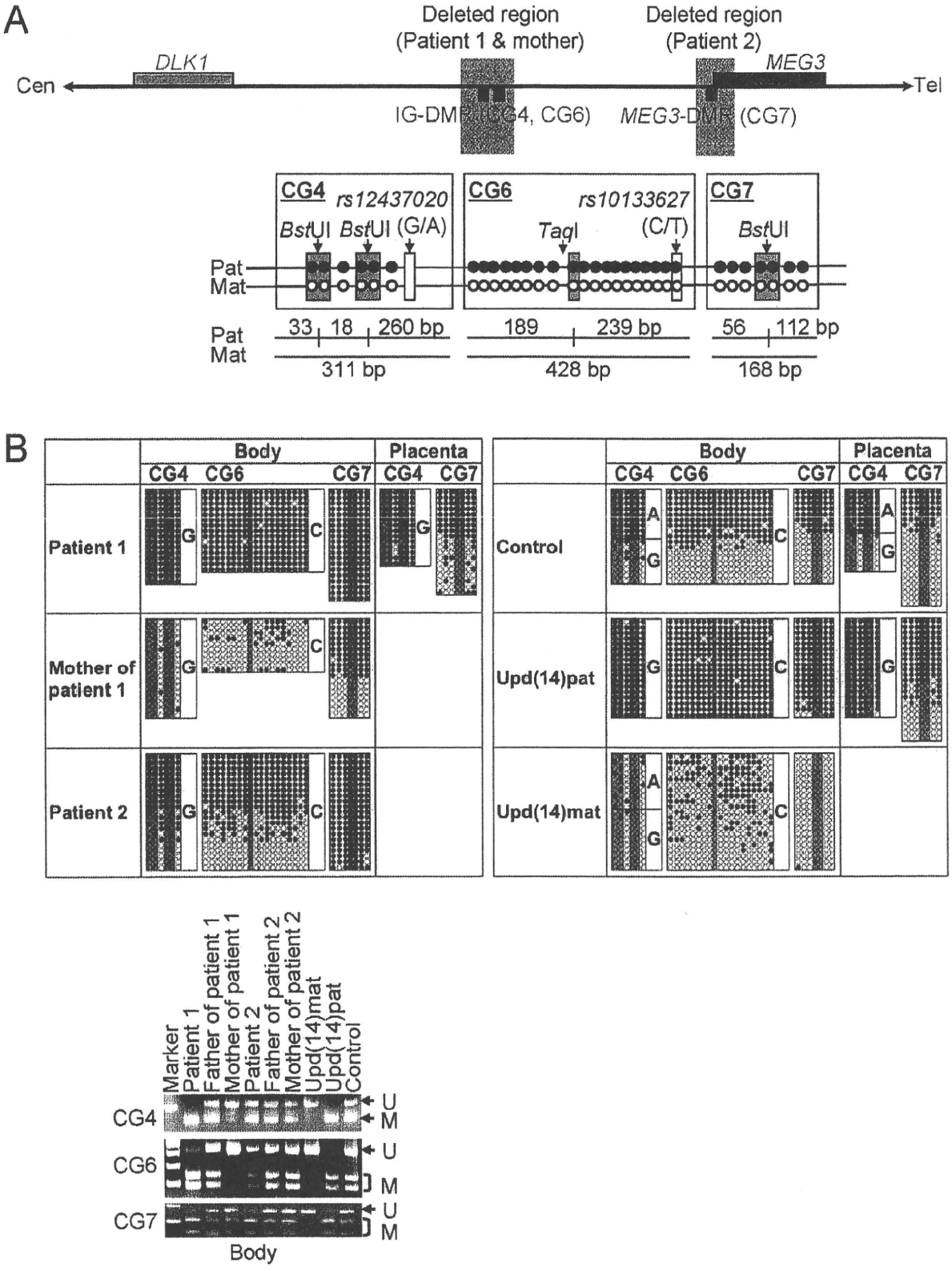

Figure 3. Methylation analysis of the IG-DMR (CG4 and CG6) and the *MEG3*-DMR (CG7). Filled and open circles indicate methylated and unmethylated cytosines at the CpG dinucleotides, respectively. (A) Structure of CG4, CG6, and CG7. Pat: paternally derived chromosome; and Mat:

maternally derived chromosome. The PCR products for CG4 (311 bp) harbor 6 CpG dinucleotides and a G/A SNP (*rs12437020*), and are digested with *Bst*UI into three fragment (33 bp, 18 bp, and 260 bp) when the cytosines at the first and the second CpG dinucleotides and the fourth and the fifth CpG dinucleotides (indicated with orange rectangles) are methylated. The PCR products for CG6 (428 bp) carry 19 CpG dinucleotides and a C/T SNP (*rs10133627*), and are digested with *Taq*I into two fragment (189 bp and 239 bp) when the cytosine at the 9th CpG dinucleotide (indicated with an orange rectangle) is methylated. The PCR products for CG7 harbor 7 CpG dinucleotides, and are digested with *Bst*UI into two fragment (56 bp and 112 bp) when the cytosines at the fourth and the fifth CpG dinucleotides (indicated with orange rectangles) are methylated. These enzymes have been utilized for combined bisulfite restriction analysis (COBRA). (B) Methylation analysis. Upper part shows bisulfite sequencing data. The SNP typing data are also denoted for CG4 and CG6. The circles highlighted in orange correspond to those shown in Figure 3A. The relatively long CG6 was not amplified from the formalin-fixed and paraffin-embedded placental samples, probably because of the degradation of genomic DNA. Note that CG4 is differentially methylated in a control placenta and is massively hypermethylated in a upd(14)pat placenta, whereas CG7 is rather hypomethylated in a upd(14)pat placenta as well as in a control placenta. Lower part shows COBRA data. U: unmethylated clone specific bands (311 bp for CG4, 428 bp for CG6, and 168 bp for CG7); and M: methylated clone specific bands (260 bp for CG4, 239 bp and 189 bp for CG6, and 112 bp and 56 bp for CG7). The results reproduce the bisulfite sequencing data, and delineate normal findings of the father of patient 1 and the parents of patient 2.
doi:10.1371/journal.pgen.1000992.g003

size was 8,558 bp (82,270,449–82,279,006 bp) for the microdeletion in patient 1 and her mother, and 4,303 bp (82,290,978–82,295,280 bp) for the microdeletion in patient 2. The microdeletion in patient 2 also involved the 5′ part of *MEG3* and five of the seven putative CTCF binding sites A–G [10], and was accompanied by insertion of a 66 bp sequence duplicated from *MEG3* intron 5 (82,299,727–82,299,792 bp on NT_026437). Direct sequencing of the exonic or transcribed regions detected no mutation in *DLK1*, *MEG3*, and *RTL1*, although several cDNA polymorphisms (cSNPs) were identified (Table S1). Oligoarray comparative genomic hybridization identified no other discernible structural abnormality (Figure S1B).

Methylation analysis of the two DMRs and the seven putative CTCF binding sites

We next studied methylation patterns of the previously reported IG-DMR (CG4 and CG6) and *MEG3*-DMR (CG7) (Figure 3A) [2], using bisulfite treated gDNA samples. Bisulfite sequencing and combined bisulfite restriction analysis using body samples revealed a hypermethylated IG-DMR and *MEG3*-DMR in patient 1, a hypomethylated IG-DMR and differentially methylated *MEG3*-DMR in the mother of patient 1, and a differentially methylated IG-DMR and hypermethylated *MEG3*-DMR in patient 2, and bisulfite sequencing using placental samples showed a hypermethylated IG-DMR and rather hypomethylated *MEG3*-DMR in patient 1 (Figure 3B).

We also examined methylation patterns of the seven putative CTCF binding sites by bisulfite sequencing (Figure 4A). The sites C and D alone exhibited DMRs in the body and were rather hypomethylated in the placenta (Figure 4B), as observed in CG7. Furthermore, to identify an informative SNP(s) pattern for allele-specific bisulfite sequencing, we examined a 349 bp region encompassing the site C and a 356 bp region encompassing the site D as well as a 300 bp region spanning the previously reported three SNPs near the site D, in 120 control subjects, the cases with upd(14)pat/mat, and patients 1 and 2 and their parents. Consequently, an informative polymorphism was identified for a novel G/A SNP near the site D in only a single control subject, and the parent-of-origin specific methylation pattern was confirmed (Figure 4C). No informative SNP was found in the examined region around the site C, and no other informative SNP was identified in the two examined regions around the site D, with the previously known three SNPs being present in a homozygous condition in all the subjects analyzed.

Expression analysis of the imprinted genes

Finally, we performed expression analyses, using standard reverse transcriptase (RT)-PCR and/or q-PCR analysis for multiple imprinted genes in this region (Figure 5A–5C). For leukocytes, weak expression was detected for *MEG3* and *SNORD114-29* in a control subject and the mother of patient 1 but not in patient 1. For skin fibroblasts, although all *MEGs* but no *PEGs* were expressed in control subjects, neither *MEGs* nor *PEGs* were expressed in patient 2. For placentas, although all imprinted genes were expressed in control subjects, *PEGs* only were expressed in patient 1. For the pituitary and adrenal of patient 2, *DLK1* expression alone was identified.

Expression pattern analyses using informative cSNPs revealed monoallelic *MEG3* expression in the leukocytes of the mother of patient 1 (Figure 5D), and biparental *RTL1* expression in the placenta of patient 1 (no informative cSNP was detected for *DLK1*) and biparental *DLK1* expression in the pituitary and adrenal of patient 2 (*RTL1* was not expressed in the pituitary and adrenal) (Figure 5E), as well as maternal *MEG3* expression in the control leukocytes and paternal *RTL1* expression in the control placentas (Figure S2). Although we also attempted q-PCR analysis, precise assessment was impossible for *MEG3* in the mother of patient 1 because of faint expression level in leukocytes and for *RTL1* in patient 1 and *DLK1* in patient 2 because of poor quality of mRNAs obtained from formalin-fixed and paraffin-embedded tissues.

Discussion

The data of the present study are summarized in Figure 6. Parental origin of the microdeletion positive chromosomes is based on the methylation patterns of the preserved DMRs in patients 1 and 2 and the mother of patient 1 as well as maternal transmission in patient 1. Loss of the hypomethylated IG-DMR of maternal origin in patient 1 was associated with epimutation (hypermethylation) of the *MEG3*-DMR in the body and caused paternalization of the imprinted region and typical upd(14)pat body and placental phenotypes, whereas loss of the hypomethylated *MEG3*-DMR of maternal origin in patient 2 permitted normal methylation pattern of the IG-DMR in the body and resulted in maternal to paternal epigenotypic alteration and typical upd(14)pat body, but no placental, phenotype. In this regard, while a 66 bp segment was inserted in patient 2, this segment contains no known regulatory sequence [11] or evolutionarily conserved element [12] (also examined with a VISTA program, http://genome.lbl.gov/vista/index.shtml). Similarly, while no control samples were available for pituitary and adrenal, the previous study in human subjects has shown paternal *DLK1* expression in adrenal as well as monoallelic *DLK1* and *MEG3* expressions in various tissues [11]. Furthermore, the present and the previous studies [2] indicate that this region is imprinted in the placenta as well as in the body. Thus, these results, in conjunction with the finding that the IG-DMR remains as a DMR and the *MEG3*-DMR exhibits a non-DMR in the placenta [2], imply the following: (1) the IG-DMR functions hierarchically as an upstream regulator for the methylation pattern of the *MEG3*-DMR on the maternally inherited chromosome in the body, but not in the placenta; (2) the hypomethylated

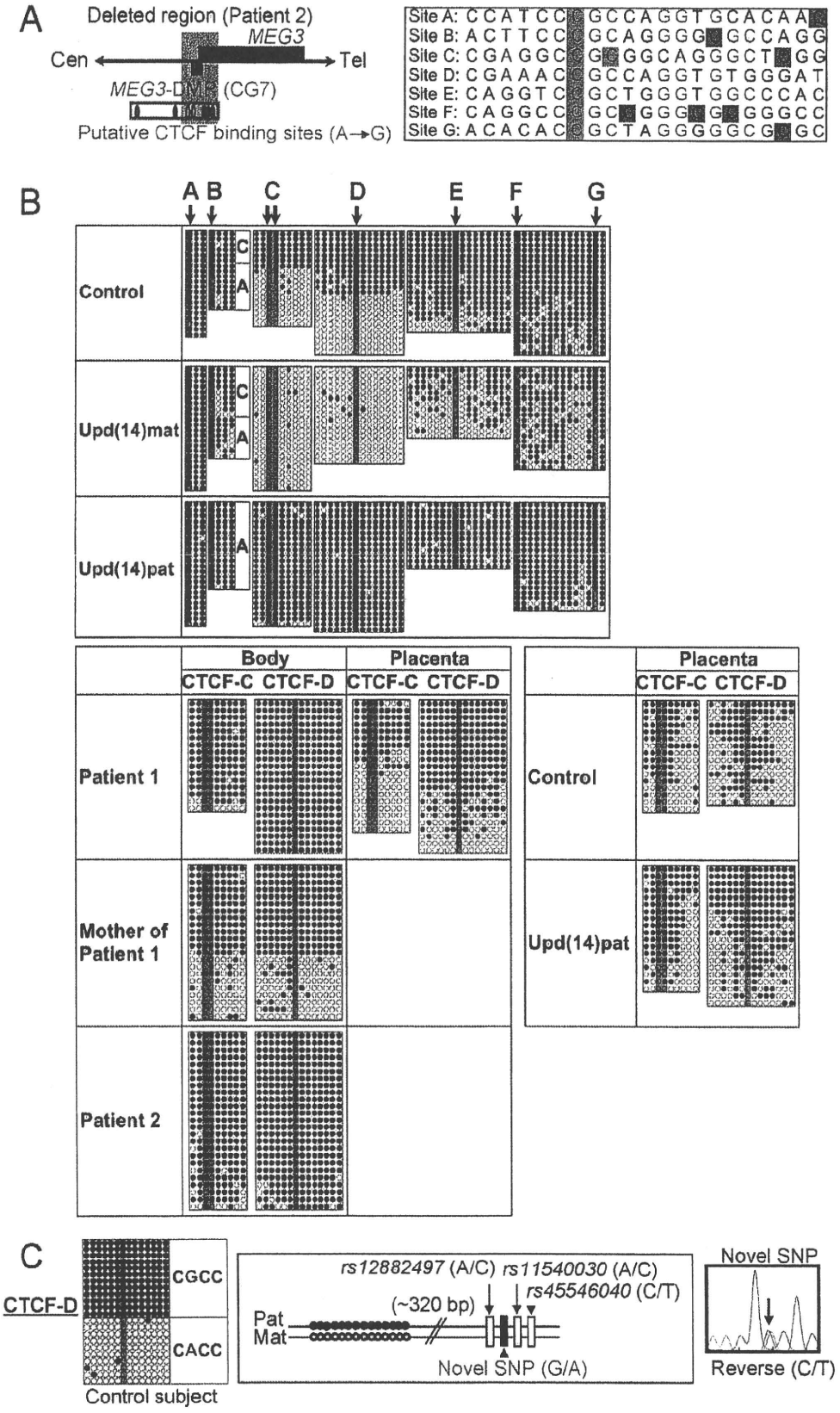
A
Deleted region (Patient 2)
MEG3
Cen
Tel
MEG3-DMR (CG7)
Putative CTCF binding sites (A→G)
Site A: C C A T C C G C C A G G T G C A C A A
Site B: A C T T C C G C A G G G G G C C A G G
Site C: C G A G G C G G G C A G G G C T G G
Site D: C G A A A C G C C A G G T G T G G G A T
Site E: C A G G T C G C T G G G T G G C C C A C
Site F: C A G G C C G C G G G G G G G C C
Site G: A C A C A C G C T A G G G G G C G G C
B
A B C D E F G
Control
Upd(14)mat
Upd(14)pat
C
A
Body
Placenta
CTCF-C CTCF-D
CTCF-C CTCF-D
Patient 1
Mother of Patient 1
Patient 2
Placenta
CTCF-C CTCF-D
Control
Upd(14)pat
C
CTCF-D
CGCC
CACC
Control subject
rs12882497 (A/C) rs11540030 (A/C)
rs45546040 (C/T)
(~320 bp)
Pat
Mat
Novel SNP (G/A)
Novel SNP
Reverse (C/T)

Figure 4. Methylation analysis of the putative CTCF protein binding sites A–G. (A) Location and sequence of the putative CTCF binding sites. In the left part, the sites C and D are painted in yellow and the remaining sites in purple. In the right part, the consensus CTCF binding motifs are shown in red letters; the cytosine residues at the CpG dinucleotides within the CTCF binding motifs are highlighted in blue, and those outside the CTCF binding motifs are highlighted in green [10]. (B) Methylation analysis. Upper part shows bisulfite sequencing data, using leukocyte genomic DNA samples. Since PCR products for the site B contain a C/A SNP (*rs11627993*), genotyping data are also indicated. The circles highlighted in blue correspond to those shown in Figure 4A. The sites C and D exhibit clear DMRs. Lower part indicates the results of the sites C and D using leukocyte and/or placental genomic DNA samples. The findings are similar to those of CG7. (C) Allele-specific methylation pattern of the CTCF binding site D. A novel G/A SNP has been identified in a single control subject, as shown on a reverse chromatogram delineating a C/T SNP pattern, while the previously reported three SNPs were present in a homozygous condition. Methylated and unmethylated clones are associated with the "G" and the "A" alleles, respectively.
doi:10.1371/journal.pgen.1000992.g004

MEG3-DMR functions as an essential imprinting regulator for both *PEGs* and *MEGs* in the body; and (3) in the placenta, the hypomethylated IG-DMR directly controls the imprinting pattern of both *PEGs* and *MEGs*. These notions also explain the epigenotypic alteration in the previous cases with epimutations or microdeletions affecting both DMRs (Figure S3).

It remains to be clarified how the IG-DMR and the *MEG3*-DMR interact hierarchically in the body. However, the present data, together with the previous findings in cases with epimutations [2,5–8], imply that *MEG3*-DMR can remain hypomethylated only in the presence of a hypomethylated IG-DMR and is methylated when the IG-DMR is deleted or methylated irrespective of the parental origin. Furthermore, mouse studies have suggested that the methylation pattern of the postfertilization-derived *Gtl2*-DMR (the mouse homolog for the *MEG3*-DMR) is dependent on that of the germline-derive IG-DMR [13]. Thus, a preferential binding of some factor(s) to the unmethylated IG-DMR may cause a conformational alteration of the genomic structure, thereby protecting the methylation of the *MEG3*-DMR.

It also remains to be elucidated how the IG-DMR and the *MEG3*-DMR regulate the expression of both *PEGs* and *MEGs* in the placenta and the body, respectively. For the *MEG3*-DMR, however, the CTCF binding sites C and D may play a pivotal role in the imprinting regulation. The methylation analysis indicates that the two sites reside within the *MEG3*-DMR, and it is known that the CTCF protein with versatile functions preferentially binds to unmethylated target sequences including the sites C and D [10,14–16]. In this regard, all the *MEGs* in this imprinted region can be transcribed together in the same orientation and show a strikingly similar tissue expressions pattern [1,12], whereas *PEGs* are transcribed in different directions and are co-expressed with *MEGs* only in limited cell-types [1,17]. It is possible, therefore, that preferential CTCF binding to the grossly unmethylated sites C and D activates all the *MEGs* as a large transcription unit and represses all the *PEGs* perhaps by influencing chromatin structure and histone modification independently of the effects of expressed *MEGs*. In support of this, CTCF protein acts as a transcriptional activator for *Gtl2* (the mouse homolog for *MEG3*) in the mouse [18].

Such an imprinting control model has not been proposed previously. It is different from the CTCF protein-mediated insulator model indicated for the *H19*-DMR and from the non-coding RNA-mediated model implicated for several imprinted regions including the KvDMR1 [19]. However, the KvDMR1 harbors two putative CTCF binding sites that may mediate non-coding RNA independent imprinting regulation [20], and the imprinting control center for Prader-Willi syndrome [21] also carries three CTCF binding sites (examined with a Search for CTCF DNA Binding Sites program, http://www.essex.ac.uk/bs/molonc/spa.html). Thus, while each imprinted region would be regulated by a different mechanism, a CTCF protein may be involved in the imprinting control of multiple regions, in various manners.

This imprinted region has also been studied in the mouse. Clinical and molecular findings in wildtype mice [1,22,23], mice with PatDi(12) (paternal disomy for chromosome 12 harboring this imprinted region) [13,24,25], and mice with targeted deletions for the IG-DMR (ΔIG-DMR) [22,26] and for the *Gtl2*-DMR (Δ*Gtl2*-DMR) [27] are summarized in Table 2. These data, together with human data, provide several informative findings. First, in both the human and the mouse, the IG-DMR is differentially methylated in both the body and the placenta, whereas the *MEG3/Gtl2*-DMR is differentially methylated in the body and exhibits non-DMR in the placenta. Second, the IG-DMR and the *MEG3/Gtl2*-DMR show a hierarchical interaction on the maternally derived chromosome in both the human and the mouse bodies. Indeed, the *MEG3/Gtl2*-DMR is epimutated in patient 1 and mice with maternally inherited ΔIG-DMR, and the IG-DMR is normally methylated in patient 2 and mice with maternally inherited Δ*Gtl2*-DMR. Third, the function of the IG-DMR is comparable between human and mouse bodies and different between human and mouse placentas. Indeed, patient 1 has upd(14)pat body and placental phenotypes, whereas mice with the ΔIG-DMR of maternal origin have PatDi(12)-compatible body phenotype and apparently normal placental phenotype. It is likely that imprinting regulation in the mouse placenta is contributed by some mechanism(s) other than the methylation pattern of the IG-DMR, such as chromatin conformation [22,28,29].

Unfortunately, however, the data of Δ*Gtl2*-DMR mice appears to be drastically complicated by the retained neomycin cassette in the upstream region of *Gtl2*. Indeed, it has been shown that the insertion of a *lacZ* gene or a neomycin gene in the similar upstream region of *Gtl2* causes severely dysregulated expression patterns and abnormal phenotypes after both paternal and maternal transmissions [30,31], and that deletion of the inserted neomycin gene results in apparently normal expression patterns and phenotypes after both paternal and maternal transmissions [31]. (In this regard, although a possible influence of the inserted 66 bp segment can not be excluded formally in patient 2, phenotype and expression data in patient 2 are compatible with simple paternalization of the imprinted region.) In addition, since the apparently normal phenotype in mice homozygous for Δ*Gtl2*-DMR is reminiscent of that in sheep homozygous for the callipyge mutation [32], a complicated mechanism(s) such as the polar overdominance may be operating in the Δ*Gtl2*-DMR mice [33]. Thus, it remains to be clarified whether the *MEG3/Gtl2*-DMR has a similar or different function between the human and the mouse.

Two points should be made in reference to the present study. First, the proposed functions of the two DMRs are based on the results of single patients. This must be kept in mind, because there might be a hidden patient-specific abnormality or event that might explain the results. For example, the abnormal placental phenotype in patient 1 might be caused by some co-incidental aberration, and the apparently normal placenta in patient 2 might be due to mosaicism with grossly preserved *MEG3*-DMR in the placenta and grossly deleted *MEG3*-DMR in the body. Second,

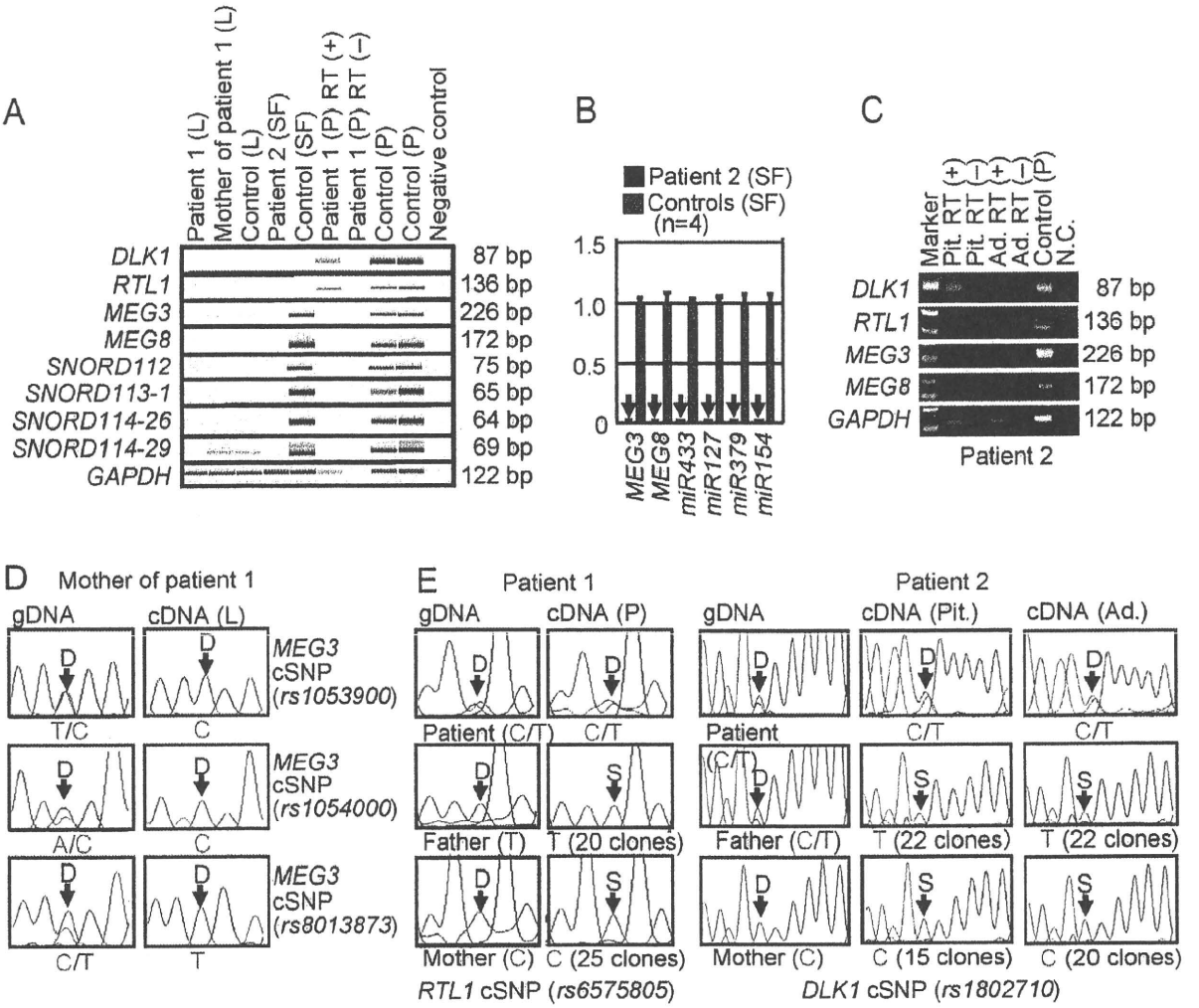

Figure 5. Expression analysis. (A) Reverse transcriptase (RT)-PCR analysis. L: leukocytes; SF: skin fibroblasts; and P: placenta. The relatively weak *GAPDH* expression for the formalin-fixed and paraffin-embedded placenta of patient 1 indicates considerable mRNA degradation. Since a single exon was amplified for *DLK1* and *RTL1*, PCR was performed with and without RT for the placenta of patient 1, to exclude the possibility of false positive results caused by genomic DNA contamination. (B) Quantitative real-time PCR (q-PCR) analysis of *MEG3*, *MEG8*, and *miRNAs*, using fresh skin fibroblasts (SF) of patient 2 and four control neonates. Of the examined *MEGs*, *miR433* and *miR127* are encoded by *RTL1as*. (C) RT-PCR analysis for the formalin-fixed and paraffin-embedded pituitary (Pit.) and the adrenal (Ad.) in patient 2. The bands for *DLK1* are detected in the presence of RT and undetected in the absence of RT, thereby excluding contamination of genomic DNA. (D) Monoallelic *MEG3* expression in the leukocytes of the mother of patient 1. The three cSNPs are present in a heterozygous status in gDNA and in a hemizygous status in cDNA. D: direct sequence. (E) Biparental *RTL1* expression in the placenta of patient 1 and biparental *DLK1* expression in the pituitary and adrenal of patient 2. D: direct sequence; and S: subcloned sequence. In patient 1, genotyping of *RTL1* cSNP (*rs6575805*) using gDNA indicates maternal origin of the "C" allele and paternal origin of the "T" allele, and sequencing analysis using cDNA confirms expression of maternally as well as paternally derived *RTL1*. Similarly, in patient 2, genotyping of *DLK1* cSNP (*rs1802710*) using gDNA denotes maternal origin of the "C" allele and paternal origin of the "T" alleles, and sequencing analysis using cDNA confirms expression of maternally as well as paternally inherited *DLK1*.
doi:10.1371/journal.pgen.1000992.g005

the clinical features in the mother of patient 1 such as short stature and obesity are often observed in cases with upd(14)mat (Table S2). However, the clinical features are non-specific and appear to be irrelevant to the microdeletion involving the IG-DMR, because loss of the paternally derived IG-DMR does not affect the imprinted status [2,26]. Indeed, *MEG3* in the mother of patient 1 showed normal monoallelic expression in the presence of the differentially methylated *MEG3*-DMR. Nevertheless, since the upd(14)mat phenotype is primarily ascribed to loss of functional *DLK1* (Figure S3B) [2,34], it might be possible that the microdeletion involving the IG-DMR has affected a *cis*-acting regulatory element for *DLK1* expression (for details, see Note in the legend for Table S2). Further studies in cases with similar microdeletions will permit clarification of these two points.

In summary, the results show a hierarchical interaction and distinct functional properties of the IG-DMR and the *MEG3*-DMR in imprinting control. Thus, this study provides significant advance in the clarification of mechanisms involved in the imprinting regulation at the 14q32.2 imprinted region and the development of upd(14) phenotype.

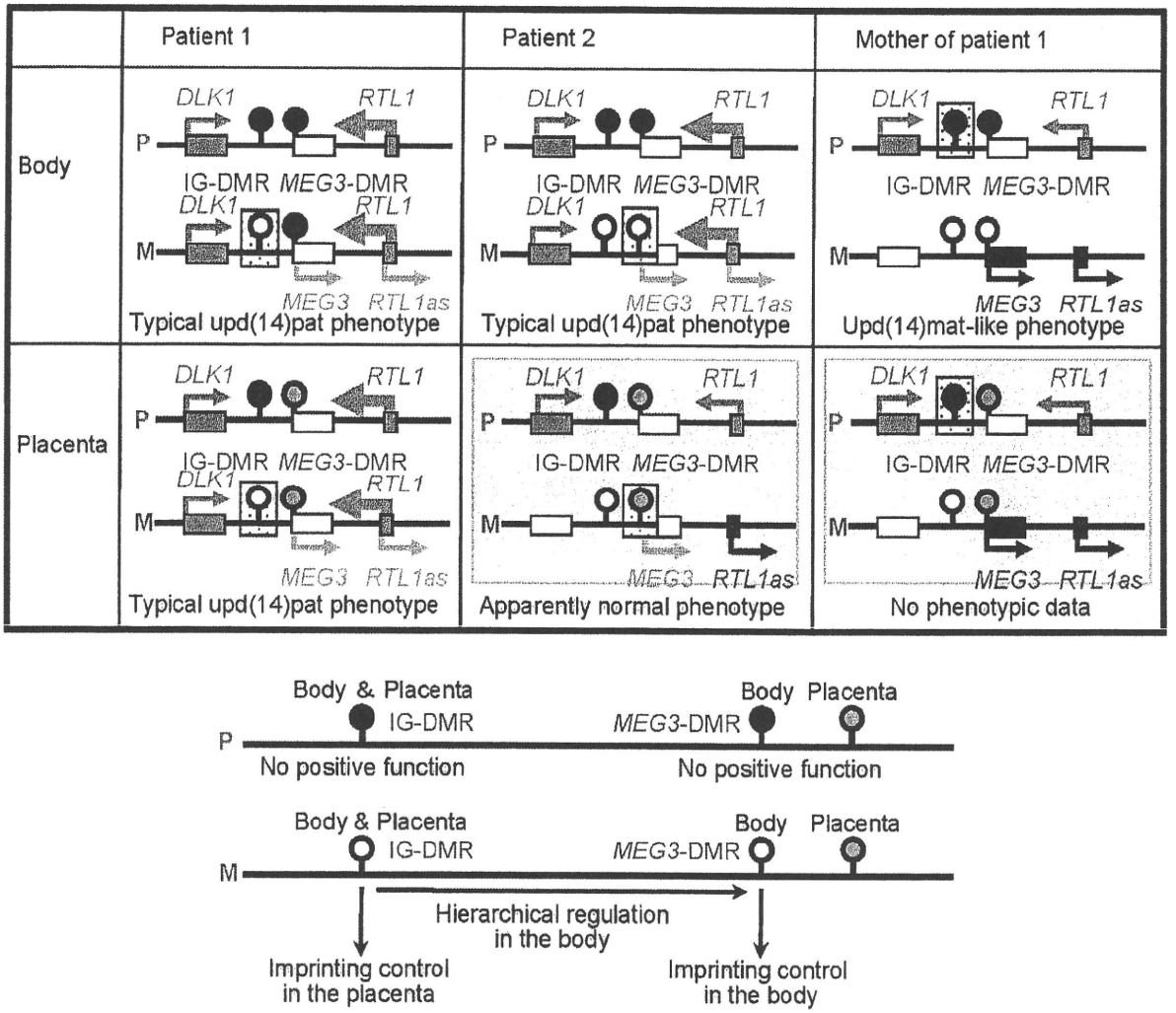

Figure 6. Schematic representation of the observed and predicted methylation and expression patterns. Deleted regions in patients 1 and 2 and the mother of patient 1 are indicated by stippled rectangles. P: paternally derived chromosome; and M: maternally derived chromosome. Representative imprinted genes are shown; these genes are known to be imprinted in the body and the placenta [2] (see also Figure S2). Placental samples have not been obtained in patient 2 and the mother of patient 1 (highlighted with light green backgrounds). Thick arrows for *RTL1* in patients 1 and 2 represent increased *RTL1* expression that is ascribed to loss of functional microRNA-containing *RTL1as* as a repressor for *RTL1* [26,36–38]; this phenomenon has been indicated in placentas with upd(14)pat and in those with an epimutation and a microdeletion involving the two DMRs (Figure S3A and S3C) [2]. *MEG3* and *RTL1as* that are disrupted or predicted to have become silent on the maternally derived chromosome are written in gray. Filled and open circles represent hypermethylated and hypomethylated DMRs, respectively; since the *MEG3*-DMR is rather hypomethylated and regarded as non-DMR in the placenta [2] (see also Figure 3), it is painted in gray.
doi:10.1371/journal.pgen.1000992.g006

Materials and Methods

Ethics statement

This study was approved by the Institutional Review Board Committees at National Center for Child health and Development, University College Dublin, and Dokkyo University School of Medicine, and performed after obtaining written informed consent.

Primers

All the primers utilized in this study are summarized in Table S3.

Sample preparation

For leukocytes and skin fibroblasts, genomic DNA (gDNA) samples were extracted with FlexiGene DNA Kit (Qiagen), and RNA samples were prepared with RNeasy Plus Mini (Qiagen) for *DLK1*, *MEG3*, *RTL1*, *MEG8* and *snoRNAs*, and with mirVana miRNA Isolation Kit (Ambion) for *microRNAs*. For paraffin-embedded tissues including the placenta, brain, lung, heart, liver, spleen, kidney, bladder, and small intestine, gDNA and RNA samples were extracted with RecoverAll Total Nucleic Acids Isolation Kit (Ambion) using slices of 40 μm thick. For fresh control placental samples, gDNA and RNA were extracted using ISOGEN (Nippon Gene). After treating total RNA samples with

Table 2. Clinical and molecular findings in wild-type and PatDi(12) mice and mice with maternally inherited ΔIG-DMR and Δ*Gtl2*-DMR.

	Wildtype	PatDi(12)	ΔIG-DMR (~4.15 kb)[a]	Δ*Gtl2*-DMR (~10 kb)[b]
				Neomycin cassette (+)
<Body>				
Phenotype	Normal	Abnormal[c]	PatDi(12) phenotype[c]	Normal at birth Lethal by 4 weeks
Methylation pattern				
IG-DMR	Differential	Methylated	Methylated[d]	Differential
Gtl2-DMR	Differential	Methylated	Epimutated[e]	Methylated[d]
Expression pattern				
Pegs	Monoallelic	Increased (~2x)	Biparental Increased (2x or 4.5x)[f]	Grossly normal
Megs	Monoallelic	Absent	Absent	Decreased (<0.2~0.5x)[g]
<Placenta>				
Phenotype	Normal	Placentomegaly	Apparently normal	Not determined
Methylation pattern				
IG-DMR	Differential	Methylated	Not determined	Not determined
Gtl2-DMR	Non-DMR	Non-DMR	Not determined	Not determined
Expression pattern				
Pegs	Monoallelic	Not determined	Increased (1.5~1.8x)[g]	Decreased (0.5~0.85x)[g]
Megs	Monoallelic	Not determined	Decreased (0.6~0.8x)[g]	Decreased (<0.1~1.0)[g]
Remark			Paternal transmission[h]	Paternal transmission[i] Biparental transmission[j]

a The deletion size is smaller than that of patient 1 and her mother in this study, especially at the centromeric region.
b The microdeletion also involves *Gtl2*, and the deletion size is larger than that of patient 2 in this study.
c Body phenotype includes bell-shaped thorax with rib anomalies, distended abdomen, and short and broad neck.
d Hemizygosity for the methylated DMR of paternal origin.
e Hypermethylation of the maternally derived DMR.
f 2x *Dlk1* and *Dio3* expression levels and 4.5x *Rtl1* expression level. The markedly elevated *Rtl1* expression level is ascribed to a synergic effect between activation of the usually silent *Rtl1* of maternal origin and loss of functional microRNA-containing *Rtl1as* as a repressor for *Rtl1* [26,36–38].
g The expression level is variable among examined tissues and examined genes.
h The ΔIG-DMR of paternal origin has permitted normal *Gtl2*-DMR methylation pattern, intact imprinting status, and normal phenotype in the body (no data on the placenta).
i The Δ*Gtl2*-DMR of paternal origin is accompanied by normal methylation pattern of the IG-DMR and variably reduced *Pegs* expression and increased *Megs* expression in the body, and has yielded severe growth retardation accompanied by perinatal lethality.
j The homozygous mutants have survived and developed into fertile adults, despite rather altered expression patterns of the imprinted genes.
doi:10.1371/journal.pgen.1000992.t002

DNase, cDNA samples for *DLK1*, *MEG3*, *MEG8*, and *snoRNAs* were prepared with oligo(dT) primers from 1 μg of RNA using Superscript III Reverse Transcriptase (Invitrogen), and those for *microRNAs* were synthesized from 300 ng of RNA using TaqMan MicroRNA Reverse Transcription Kit (Applied Biosystems). For *RTL1*, cDNA samples were synthesized with *RTL1*-specific primers that do not amplify *RTL1as*. Control gDNA and cDNA samples were extracted from adult leukocytes and neonatal skin fibroblasts purchased from Takara Bio Inc. Japan, and from a fresh placenta of 38 weeks of gestation. Metaphase spreads were prepared from leukocytes and skin fibroblasts using colcemide (Invitrogen).

Structural analysis

Microsatellite analysis and SNP genotyping were performed as described previously [2]. For FISH analysis, metaphase spreads were hybridized with a 5,104 bp FISH-1 probe and a 5,182 bp FISH-2 probe produced by long PCR, together with an RP11-566I2 probe for 14q12 used as an internal control [2]. The FISH-1 and FISH-2 probes were labeled with digoxigenin and detected by rhodamine anti-digoxigenin, and the RP11-566I2 probe was labeled with biotin and detected by avidin conjugated to fluorescein isothiocyanate. For quantitative real-time PCR analysis, the relative copy number to RNaseP (catalog No: 4316831, Applied Biosystems) was determined by the Taqman real-time PCR method using the probe-primer mix on an ABI PRISM 7000 (Applied Biosystems). To determine the breakpoints of microdeletions, sequence analysis was performed for long PCR products harboring the fusion points, using serial forward primers on the CEQ 8000 autosequencer (Beckman Coulter). Direct sequencing was also performed on the CEQ 8000 autosequencer. Oligoarray comparative genomic hybridization was performed with 1×244K Human Genome Array (catalog No: G4411B) (Agilent Technologies), according to the manufacturer's protocol.

Methylation analysis

Methylation analysis was performed for gDNA treated with bisulfite using the EZ DNA Methylation Kit (Zymo Research). After PCR amplification using primer sets that hybridize both methylated and unmethylated clones because of lack of CpG

dinucleotides within the primer sequences, the PCR products were digested with appropriate restriction enzymes for combined bisulfite restriction analysis. For bisulfite sequencing, the PCR products were subcloned with TOPO TA Cloning Kit (Invitrogen) and subjected to direct sequencing on the CEQ 8000 autosequencer.

Expression analysis

Standard RT-PCR was performed for *DLK1*, *RTL1*, *MEG3*, *MEG8*, and *snoRNAs* using primers hybridizing to exonic or transcribed sequences, and one µl of PCR reaction solutions was loaded onto Gel-Dye Mix (Agilent). Taqman real-time PCR was carried out using the probe-primer mixtures (assay No: Hs00292028 for *MEG3* and Hs00419701 for *MEG8*; assay ID: 001028 for *miR433*, 000452 for *miR127*, 000568 for *miR379*, and 000477 for *miR154*) on the ABI PRISM 7000. Data were normalized against *GAPDH* (catalog No: 4326317E) for *MEG3* and *MEG8* and against *RNU48* (assay ID: 0010006) for the remaining *miRs*. The expression studies were performed three times for each sample.

To examine the imprinting status of *MEG3* in the leukocytes of the mother of patient 1, direct sequence data for informative cSNPs were compared between gDNA and cDNA. To analyze the imprinting status of *RTL1* in the placental sample of patient 1 and that of *DLK1* in the pituitary and adrenal samples of patient 2, RT-PCR products containing exonic cSNPs informative for the parental origin were subcloned with TOPO TA Cloning Kit, and multiple clones were subjected to direct sequencing on the CEQ 8000 autosequencer. Furthermore, *MEG3* expression pattern was examined using leukocyte gDNA and cDNA samples from multiple normal subjects and leukocyte gDNA samples from their mothers, and *RTL1* expression pattern was analyzed using gDNA and cDNA samples from multiple fresh normal placentas and leukocyte gDNA from the mothers.

Supporting Information

Figure S1 Structural analysis. (A) Quantitative real-time PCR analysis (q-PCR) for four regions (q-PCR-1-4) in patient 2. The q-PCR-1 and q-PCR-2 regions are present in two copies whereas q-PCR-3 and q-PCR-4 regions are present in a single copy in patient 2. The four regions are present in two copies in the parents and a control subject, in a single copy in the two previously reported patients with microdeletions involving the examined regions (Deletion-1 and Deletion-2 are case 2 and case 3 in Kagami et al. [2], respectively), and in three copies in a hitherto unreported case with 46,XX,der(17)t(14;17)(q32.2;p13)pat who have three copies of the 14q32.2 imprinted region. Since the microsatellite locus *D14S985* is present in two copies (Table S1) and the *MEG3*-DMR is deleted (Figure 2) in patient 2, this has served to localize the breakpoints. (B) Oligoarray comparative genomic hybridization for a ~1 Mb imprinted region. All the signals remain within the normal range (-1 SD ~ +1 SD) (shaded in light blue) in patients 1 and 2.
Found at: doi:10.1371/journal.pgen.1000992.s001 (1.17 MB TIF)

Figure S2 Expression analysis. (A) Maternal *MEG3* expression in the leukocytes of normal subjects. Genotyping has been performed for three cSNPs using genomic DNA (gDNA) and cDNA of leukocytes from control subjects and gDNA samples of their mothers, indicating that both maternally and non-maternally (paternally) derived alleles are delineated in the gDNA, whereas maternally inherited alleles alone are identified in cDNA. These three cSNPs have also been studied in the mother of patient 1 (Figure 5D). (B) Paternal *RTL1* expression in the placenta of a normal subject. Genotyping has been carried out for *RTL1* cSNP using gDNA and cDNA samples of a fresh placenta and gDNA sample from the mother, showing that both maternally and non-maternally (paternally) derived alleles are delineated in the gDNA, whereas a non-maternally (paternally) inherited allele alone is detected in cDNA. This cSNP has also been examined in the placenta of patient 1 (Figure 5E). Furthermore, the results confirm that the primers utilized in this study have amplified *RTL1*, but not *RTL1as*.
Found at: doi:10.1371/journal.pgen.1000992.s002 (0.39 MB TIF)

Figure S3 Schematic representation of the observed and predicted methylation and expression patterns in previously reported cases with upd(14)pat/mat-like phenotypes and in normal and upd(14)pat/mat subjects. For the explanations of the illustrations, see the legend for Figure 6. Previous studies have indicated that (1) Epimutation-1, Deletion-1, Deletion-2, and Deletion-3 lead to maternal to paternal epigenotypic alteration; (2) Epimutation-2 results in paternal to maternal epigenotypic alteration; and (3) Deletion-4 and Deletion-5 have no effect on the epigenotypic status [2,5–8,26]. (A) Cases with typical or mild upd(14)pat phenotype. Epimutation-1: Hypermethylation of the IG-DMR and the *MEG3*-DMR of maternal origin in the body, and that of the IG-DMR of maternal origin in the placenta (the *MEG3*-DMR is rather hypomethylated in the placenta) (cases 6–8 in Kagami et al. [2]). Deletion-1: Microdeletion involving *DLK1*, the two DMRs, and *MEG3* on the maternally inherited chromosome (case 2 in Kagami et al. [2]). Deletion-2: Microdeletion involving *DLK1*, the two DMRs, *MEG3*, *RTL1*, and *RTL1as* on the maternally inherited chromosome (cases 3 and 5 in Kagami et al. [2]). Deletion-3: Microdeletion involving the two DMRs, *MEG3*, *RTL1*, and *RTL1as* on the maternally inherited chromosome (case 4 in Kagami et al. [2]). These findings are explained by the following notions: (1) Epimutation (hypermethylation) of the normally hypomethylated IG-DMR of maternal origin directly results in paternalization of the imprinted region in the placenta and indirectly leads to paternalization of the imprinted region in the body via epimutation (hypermethylation) of the usually hypomethylated *MEG3*-DMR of maternal origin. Thus, the epimutation (hypermethylation) is predicted to have impaired the IG-DMR as the primary target, followed by the epimutation (hypermethylation) of the *MEG3*-DMR after fertilization; (2) Loss of the hypomethylated *MEG3*-DMR of maternal origin leads to paternalization of the imprinted region in the body; and (3) Loss of the hypomethylated IG-DMR of maternal origin results in paternalization of the imprinted region in the placenta. Furthermore, epigenotype-phenotype correlations imply that the severity of upd(14)pat phenotype is primarily determined by the *RTL1* expression dosage rather than the *DLK1* expression dosage [2]. (B) Cases with upd(14)mat-like phenotype. Epimutation-2: Hypomethylation of the IG-DMR and the *MEG3*-DMR of paternal origin (Temple et al. [5], Buiting et al. [6], Hosoki et al. [7], and Zechner et al. [8]). Deletion-4: Microdeletion involving *DLK1*, the two DMRs, and *MEG3* on the paternally inherited chromosome (cases 9 and 10 in Kagami et al. [2]). Deletion-5: Microdeletion involving *DLK1*, the two DMRs, *MEG3*, *RTL1*, and *RTL1as* on the paternally inherited chromosome (case 11 in Kagami et al. [2] and patient 3 in Buiting et al. [6]). These findings are consistent with the following notions: (1) Epimutation (hypomethylation) of the normally hypermethylated IG-DMR of paternal origin directly results in maternalization of the imprinted region in the placenta and indirectly leads to maternalization of the imprinted region in the body through epimutation (hypomethylation) of the usually hypermethylated *MEG3*-DMR of paternal origin. Thus, epimutation (hypomethylation) is predicted to have affected the IG-DMR

as the primary target, followed by the epimutation (hypomethylation) of the *MEG3*-DMR after fertilization; and (2) Loss of the hypermethylated DMRs of paternal origin has no effect on the imprinting status [2,26], so that upd(14)mat-like phenotype is primarily ascribed to the additive effects of loss of functional *DLK1* and *RTL1* from the paternally derived chromosome (the effects of loss of *DIO3* appears to be minor, if any [2,35]). Although the *MEGs* expression dosage is predicted to be normal in Deletion-4 and Deletion-5 and doubled in Epimutation-2 as well as in upd(14)mat, it remains to be determined whether the difference in the *MEGs* expression dosage has major clinical effects or not. (C) Normal and upd(14)pat/mat subjects.
Found at: doi:10.1371/journal.pgen.1000992.s003 (2.72 MB TIF)

Table S1 The results of microsatellite and SNP analyses.
Found at: doi:10.1371/journal.pgen.1000992.s004 (0.19 MB DOC)

Table S2 Clinical features in the mother of patient 1.
Found at: doi:10.1371/journal.pgen.1000992.s005 (0.09 MB DOC)

Table S3 Primers utilized in the present study.
Found at: doi:10.1371/journal.pgen.1000992.s006 (0.14 MB DOC)

Author Contributions

Conceived and designed the experiments: MK ACFS TO. Performed the experiments: MK MF KM FK. Analyzed the data: MK TO. Contributed reagents/materials/analysis tools: MJO AJG YW OA NM KM TO. Wrote the paper: TO.

References

1. da Rocha ST, Edwards CA, Ito M, Ogata T, Ferguson-Smith AC (2008) Genomic imprinting at the mammalian Dlk1-Dio3 domain. Trends Genet 24: 306–316.
2. Kagami M, Sekita Y, Nishimura G, Irie M, Kato F, et al. (2008) Deletions and epimutations affecting the human 14q32.2 imprinted region in individuals with paternal and maternal upd(14)-like phenotypes. Nat Genet 40: 237–242.
3. Kagami M, Yamazawa K, Matsubara K, Matsuo N, Ogata T (2008) Placentomegaly in paternal uniparental disomy for human chromosome 14. Placenta 29: 760–761.
4. Kotzot D (2004) Maternal uniparental disomy 14 dissection of the phenotype with respect to rare autosomal recessively inherited traits, trisomy mosaicism, and genomic imprinting. Ann Genet 47: 251–260.
5. Temple IK, Shrubb V, Lever M, Bullman H, Mackay DJ (2007) Isolated imprinting mutation of the DLK1/GTL2 locus associated with a clinical presentation of maternal uniparental disomy of chromosome 14. J Med Genet 44: 637–640.
6. Buiting K, Kanber D, Martin-Subero JI, Lieb W, Terhal P, et al. (2008) Clinical features of maternal uniparental disomy 14 in patients with an epimutation and a deletion of the imprinted DLK1/GTL2 gene cluster. Hum Mutat 29: 1141–1146.
7. Hosoki K, Ogata T, Kagami M, Tanaka T, Saitoh S (2008) Epimutation (hypomethylation) affecting the chromosome 14q32.2 imprinted region in a girl with upd(14)mat-like phenotype. Eur J Hum Genet 16: 1019–1023.
8. Zechner U, Kohlschmidt N, Rittner G, Damatova N, Beyer V, et al. (2009) Epimutation at human chromosome 14q32.2 in a boy with a upd(14)mat-like clinical phenotype. Clin Genet 75: 251–258.
9. Li E, Beard C, Jaenisch R (1993) Role for DNA methylation in genomic imprinting. Nature 366: 362–365.
10. Rosa AL, Wu YQ, Kwabi-Addo B, Coveler KJ, Reid Sutton V, et al. (2005) Allele-specific methylation of a functional CTCF binding site upstream of MEG3 in the human imprinted domain of 14q32. Chromosome Res 13: 809–818.
11. Wylie AA, Murphy SK, Orton TC, Jirtle RL (2000) Novel imprinted DLK1/GTL2 domain on human chromosome 14 contains motifs that mimic those implicated in IGF2/H19 regulation. Genome Res 10: 1711–1718.
12. Tierling S, Dalbert S, Schoppenhorst S, Tsai CE, Oliger S, et al. (2007) High-resolution map and imprinting analysis of the Gtl2-Dnchc1 domain on mouse chromosome 12. Genomics 87: 225–235.
13. Takada S, Paulsen M, Tevendale M, Tsai CE, Kelsey G, et al. (2002) Epigenetic analysis of the Dlk1-Gtl2 imprinted domain on mouse chromosome 12: implications for imprinting control from comparison with Igf2-H19. Hum Mol Genet 11: 77–86.
14. Ohlsson R, Renkawitz R, Lobanenkov V (2001) CTCF is a uniquely versatile transcription regulator linked to epigenetics and disease. Trends Genet 17: 520–527.
15. Hark AT, Schoenherr CJ, Katz DJ, Ingram RS, Levorse JM, et al. (2000) CTCF mediates methylation-sensitive enhancer-blocking activity at the H19/Igf2 locus. Nature 405: 486–489.
16. Kanduri C, Pant V, Loukinov D, Pugacheva E, Qi CF, et al. (2000) Functional association of CTCF with the insulator upstream of the H19 gene is parent of origin-specific and methylation-sensitive. Curr Biol 10: 853–856.
17. da Rocha ST, Tevendale M, Knowles E, Takada S, Watkins M, et al. (2007) Restricted co-expression of Dlk1 and the reciprocally imprinted non-coding RNA, Gtl2: implications for cis-acting control. Dev Biol 306: 810–823.
18. Wan LB, Pan H, Hannenhalli S, Cheng Y, Ma J, et al. (2008) Maternal depletion of CTCF reveals multiple functions during oocyte and preimplantation embryo development. Development 135: 2729–2738.
19. Ideraabdullah FY, Vigneau S, Bartolomei MS (2008) Genomic imprinting mechanisms in mammals. Mutat Res 647: 77–85.
20. Fitzpatrick GV, Pugacheva EM, Shin JY, Abdullaev Z, Yang Y, et al. (2007) Allele-specific binding of CTCF to the multipartite imprinting control region KvDMR1. Mol Cell Biol 27: 2636–2647.
21. Horsthemke B, Wagstaff J (2008) Mechanisms of imprinting of the Prader-Willi/Angelman region. Am J Med Genet A 146A: 2041–2052.
22. Lin SP, Coan P, da Rocha ST, Seitz H, Cavaille J, et al. (2007) Differential regulation of imprinting in the murine embryo and placenta by the Dlk1-Dio3 imprinting control region. Development 134: 417–426.
23. Coan PM, Burton GJ, Ferguson-Smith AC (2005) Imprinted genes in the placenta–a review. Placenta 26 Suppl A: S10–20.
24. Georgiades P, Watkins M, Surani MA, Ferguson-Smith AC (2000) Parental origin-specific developmental defects in mice with uniparental disomy for chromosome 12. Development 127: 4719–4728.
25. Takada S, Tevendale M, Baker J, Georgiades P, Campbell E, et al. (2000) Delta-like and gtl2 are reciprocally expressed, differentially methylated linked imprinted genes on mouse chromosome 12. Curr Biol 10: 1135–1138.
26. Lin SP, Youngson N, Takada S, Seitz H, Reik W, et al. (2003) Asymmetric regulation of imprinting on the maternal and paternal chromosomes at the Dlk1-Gtl2 imprinted cluster on mouse chromosome 12. Nat Genet 35: 97–102.
27. Takahashi N, Okamoto A, Kobayashi R, Shirai M, Obata Y, et al. (2009) Deletion of Gtl2, imprinted non-coding RNA, with its differentially methylated region induces lethal parent-origin-dependent defects in mice. Hum Mol Genet 18: 1879–1888.
28. Lewis A, Mitsuya K, Umlauf D, Smith P, Dean W, et al. (2004) Imprinting on distal chromosome 7 in the placenta involves repressive histone methylation independent of DNA methylation. Nat Genet 36: 1291–1295.
29. Umlauf D, Goto Y, Cao R, Cerqueira F, Wagschal A, et al. (2004) Imprinting along the Kcnq1 domain on mouse chromosome 7 involves repressive histone methylation and recruitment of Polycomb group complexes. Nat Genet 36: 1296–1300.
30. Sekita Y, Wagatsuma H, Irie M, Kobayashi S, Kohda T, et al. (2006) Aberrant regulation of imprinted gene expression in Gtl2lacZ mice. Cytogenet. Genome Res 113: 223–229.
31. Steshina EY, Carr MS, Glick EA, Yevtodiyenko A, Appelbe OK, et al. (2006) Loss of imprinting at the Dlk1-Gtl2 locus caused by insertional mutagenesis in the Gtl2 5′ region. BMC Genet 7: 44.
32. Charlier C, Segers K, Karim L, Shay T, Gyapay G, et al. (2001) The callipyge mutation enhances the expression of coregulated imprinted genes in cis without affecting their imprinting status. Nat Genet 27: 367–369.
33. Georges M, Charlier C, Cockett N (2003) The callipyge locus: evidence for the trans interaction of reciprocally imprinted genes. Trends Genet 19: 248–252.
34. Moon YS, Smas CM, Lee K, Villena JA, Kim KH, et al. (2002) Mice lacking paternally expressed Pref-1/Dlk1 display growth retardation and accelerated adiposity. Mol Cell Biol 22: 5585–5592.
35. Tsai CE, Lin SP, Ito M, Takagi N, Takada S, et al. (2002) Genomic imprinting contributes to thyroid hormone metabolism in the mouse embryo. Curr Biol 12: 1221–1226.
36. Sekita Y, Wagatsuma H, Nakamura K, Ono R, Kagami M, et al. (2008) Role of retrotransposon-derived imprinted gene, Rtl1, in the feto-maternal interface of mouse placenta. Nat Genet 40: 243–248.
37. Seitz H, Youngson N, Lin SP, Dalbert S, Paulsen M, et al. (2003) Imprinted microRNA genes transcribed antisense to a reciprocally imprinted retrotransposon-like gene. Nat Genet 34: 261–262.
38. Davis E, Caiment F, Tordoir X, Cavaillé J, Ferguson-Smith A, et al. (2005) RNAi-mediated allelic trans-interaction at the imprinted Rtl1/Peg11 locus. Curr Biol 15: 743–749.

JMG Online First, published on August 3, 2010 as 10.1136/jmg.2010.079343

Parthenogenetic chimaerism/mosaicism with a Silver-Russell syndrome-like phenotype

K Yamazawa,[1,2] K Nakabayashi,[3] M Kagami,[1] T Sato,[1] S Saitoh,[4] R Horikawa,[5] N Hizuka,[6] T Ogata[1]

► Additional figures, tables and an appendix are published online only. To view these files, please visit the journal online (http://jmg.bmj.com).

[1]Departments of Endocrinology and Metabolism, National Research Institute for Child Health and Development, Tokyo, Japan
[2]Department of Physiology, Development & Neuroscience, University of Cambridge, Cambridge, UK
[3]Maternal-Fetal Biology, National Research Institute for Child Health and Development, Tokyo, Japan
[4]Department of Pediatrics, Hokkaido University Graduate School of Medicine, Sapporo, Japan
[5]Division of Endocrinology and Metabolism, National Children's Hospital, Tokyo, Japan
[6]Department of Medicine, Institute of Clinical Endocrinology, Tokyo Women's Medical University, Tokyo, Japan

Correspondence to
Dr Tsutomu Ogata, Department of Endocrinology and Metabolism, National Research Institute for Child Health and Development, 2-10-1 Ohkura, Setagaya, Tokyo 157-8535, Japan; tomogata@nch.go.jp

Received 20 March 2010
Revised 6 May 2010
Accepted 8 May 2010

ABSTRACT

Introduction We report a 34-year-old Japanese female with a Silver-Russell syndrome (SRS)-like phenotype and a mosaic Turner syndrome karyotype (45,X/46,XX).

Methods/Results Molecular studies including methylation analysis of 17 differentially methylated regions (DMRs) on the autosomes and the *XIST*-DMR on the X chromosome and genome-wide microsatellite analysis for 96 autosomal loci and 30 X chromosomal loci revealed that the 46,XX cell lineage was accompanied by maternal uniparental isodisomy for all chromosomes (upid(AC)mat), whereas the 45,X cell lineage was associated with biparentally derived autosomes and a maternally derived X chromosome. The frequency of the 46,XX upid(AC)mat cells was calculated as 84% in leukocytes, 56% in salivary cells, and 18% in buccal epithelial cells.

Discussion The results imply that a parthenogenetic activation took place around the time of fertilisation of a sperm missing a sex chromosome, resulting in the generation of the upid(AC)mat 46,XX cell lineage by endoreplication of one blastomere containing a female pronucleus and the 45,X cell lineage by union of male and female pronuclei. It is likely that the extent of overall (epi)genetic aberrations exceeded the threshold level for the development of SRS phenotype, but not for the occurrence of other imprinting disorders or recessive Mendelian disorders.

Although a mammal with maternal uniparental disomy for all chromosomes (upd(AC)mat) is incompatible with life because of genomic imprinting,[1] a mammal with a upd(AC)mat cell lineage could be viable in the presence of a co-existing normal cell lineage. In the human, Strain *et al*[2] have reported 46,XX peripheral blood cells with maternal uniparental isodisomy for all chromosomes (upid(AC)mat) in a 1.2-year-old phenotypically male patient with aggressive behaviour, hemifacial hypoplasia and normal birth weight. Because of the 46,XX disorders of sex development, detailed molecular studies were performed, revealing the presence of a normal 46,XY cell lineage in a vast majority of skin fibroblasts and a upid(AC)mat 46,XX cell lineage in nearly all blood cells. In addition, although the data are insufficient to draw a definitive conclusion, Horike *et al*[3] have also identified 46,XX peripheral blood cells with possible upd(AC)mat in a phenotypically male patient through methylation analyses for plural differentially methylated regions (DMRs) in 11 patients with Silver–Russell syndrome (SRS)-like phenotype. This patient was found to have a normal 46,XY cell lineage and a triploid 69,XXY cell lineage in skin fibroblasts.

However, such patients with a upd(AC)mat cell lineage remain extremely rare, and there is no report describing a human with such a cell lineage in the absence of a normal cell lineage. Here, we report a female patient with a upid(AC)mat 46,XX cell lineage and a non-upd 45,X cell lineage who was identified through genetic screenings of 103 patients with SRS-like phenotype.

MATERIALS AND METHODS

Case report

This Japanese female patient was conceived naturally and born at 40 weeks of gestation by a normal vaginal delivery. At birth, her length was 44.0 cm (−3.1 SD), her weight 2.1 kg (−2.9 SD) and her occipitofrontal head circumference (OFC) 30.5 cm (−2.3 SD). The parents and the younger brother were clinically normal (the father died from a traffic accident).

At 2 years of age, she was referred to us because of growth failure. Her height was 77.7 cm (−2.5 SD), her weight 8.45 kg (−2.6 SD) and her OFC 43.5 cm (−2.5 SD). Physical examination revealed several SRS-like somatic features such as triangular face, right hemihypoplasia and bilateral fifth finger clinodactyly. She also had developmental retardation, with a developmental quotient of 56. Endocrine studies for short stature were normal as were radiological studies. Cytogenetic analysis using lymphocytes indicated a low-grade mosaic Turner syndrome (TS) karyotype, 45,X[3]/46,XX[47]. Thus, a screening of TS phenotype[4] was performed, detecting horseshoe kidney but no body surface features or cardiovascular lesion. Chromosome analysis was repeated at 6 and 32 years of age using lymphocytes, revealing a 45,X[8]/46,XX[92] karyotype and a 45,X[12]/46,XX[88] karyotype, respectively. On the last examination at 34 years of age, her height was 125.0 cm (−6.2 SD), her weight 37.5 kg (−2.0 SD) and her OFC 51.2 cm (−2.8 SD). She was engaged in a simple work and was able to get on her daily life for herself.

Sample preparation

This study was approved by the Institutional Review Board Committees at National Center for Child health and Development. After obtaining written informed consent, genomic DNA was extracted from leukocytes of the patient, the mother and the brother and from salivary cells, which comprise ~40% of buccal epithelial cells and ~60% of leukocytes,[5] of the patient. Lymphocyte metaphase spreads and leukocyte RNA were also

obtained from the patient. Leukocytes of healthy adults and patients with imprinting disorders were utilised for controls.

Primers and probes

The primers utilised in this study are summarised in supplementary methods and supplementary tables 1–3.

DMR analyses

We first performed bio-combined bisulfite restriction analysis (COBRA)[6] and bisulfite sequencing of the *H19*-DMR (A) on chromosome 11p15.5 by the previously described methods[7] and methylation-sensitive PCR analysis of the *MEST*-DMR (A) on chromosome 7q32.2 by the previously described methods[8] with minor modifications (the methylated and unmethylated allele-specific primers were designed to yield PCR products of different sizes, and the PCR products were visualised on the 2100 Bioanalyzer (Agilent, Santa Clara, California, USA)). This was because hypomethylation (epimutation) of the normally methylated *H19*-DMR of paternal origin and maternal uniparental disomy 7 are known to account for 35–65% and 5–10% of SRS patients, respectively.[9 10] In addition, fluorescence in situ hybridisation (FISH) analysis was performed with a ~84-kb RP5-998N23 probe containing the *H19*-DMR (BACPAC Resources Center, Oakland, California, USA). We also examined multiple other DMRs by bio-COBRA. The ratio of methylated clones (the methylation index) was calculated using peak heights of digested and undigested fragments on the 2100 Bioanalyzer using 2100 expert software.

Genome-wide microsatellite analysis

Microsatellite analysis was performed for 96 autosomal loci and 30 X chromosomal loci. The segment encompassing each locus was PCR-amplified, and the PCR product size was determined on the ABI PRISM 310 autosequencer using GeneScan software (Applied Biosystems, Foster City, California, USA).

PCR analysis for Y chromosomal loci

Standard PCR was performed for six Y chromosomal loci. The PCR products were electrophoresed using the 2100 Bioanalyzer.

Expression analysis

Quantitative real-time reverse transcriptase PCR analysis was performed for three paternally expressed genes (*IGF2*, *SNRPN* and *ZAC1*) and four maternally expressed genes (*H19*, *MEG3*, *PHLDA2* and *CDKN1C*) that are known to be variably (usually weakly) expressed in leukocytes (UniGene, http://www.ncbi.nlm.nih.gov/sites/entrez?db=unigene), using an ABI Prism 7000 Sequence Detection System (Applied Biosystems). *TBP* and *GAPDH* were utilised as internal controls.

RESULTS

DMR analyses

In leukocytes, the bio-COBRA indicated severely hypomethylated *H19*-DMR, and bisulfite sequencing combined with *rs2251375* SNP typing for 30 clones revealed maternal origin of 29 hypomethylated clones and non-maternal (paternal) origin of a single methylated clone in this patient (figure 1A). Thus, the marked hypomethylation of the *H19*-DMR was caused by predominance of maternally derived clones rather than hypomethylation of the *H19*-DMR of paternal origin. FISH analysis for 100 lymphocyte metaphase spreads excluded an apparent deletion of the paternally derived *H19*-DMR or duplication of the maternally derived *H19*-DMR (Supplementary figure 1). Methylation-sensitive PCR amplification for the *MEST*-DMR delineated a major peak for the methylated allele and a minor peak for the unmethylated allele (figure 1B). This also indicated the predominance of maternally derived clones and the co-existence of a minor portion of paternally derived clones. Furthermore, autosomal DMRs invariably exhibited markedly abnormal methylation patterns consistent with predominance of maternally inherited DMRs, whereas the methylation index of the *XIST*-DMR on the X chromosome remained within the female reference range (figure 1C). The abnormal methylation patterns were less obvious in salivary cells (thus, in buccal epithelial cells) than in leukocytes, except for the methylation index for the *XIST*-DMR that mildly exceeded the female reference range (figure 1A–C).

Microsatellite analysis

Major peaks consistent with maternal uniparental isodisomy and minor peaks of non-maternal (paternal) origin were identified for at least one locus on each autosome, with the minor peaks of non-maternal origin being more obvious in salivary cells than in leukocytes (figure 1D and supplementary table 4). Furthermore, the frequency of the upid(AC)mat cells was calculated as 84% in leukocytes, 56% in salivary cells and 18% in epithelial buccal cells, using the area under curves for the maternally and the non-maternally inherited peaks (supplementary note). Such minor peaks of non-maternal origin were not detected for all the 30 X chromosomal loci examined.

PCR analysis for Y chromosomal loci

PCR amplification failed to detect any trace of Y chromosome-specific bands in leukocytes and salivary cells (Supplementary figure 2).

Expression analysis

Expression analysis using control leukocytes indicated that, of the seven examined genes, *SNRPN* expression alone was strong enough to allow for a precise assessment (Supplementary figure 3). *SNRPN* expression was extremely low in this patient (figure 1E).

DISCUSSION

These results imply that this patient had a upid(AC)mat 46,XX cell lineage and a non-upd 45,X cell lineage. Indeed, methylation patterns of the *XIST*-DMR is explained by assuming that the two X chromosomes in the upid(AC)mat cells undergo random X-inactivation and that 45,X cells with the methylated *XIST*-DMR on a single active X chromosome[11] are relatively prevalent in buccal epithelial cells. Furthermore, lack of non-maternally derived minor peaks for microsatellite loci on the X chromosome is explained by assuming that the two X chromosomes in the upid(AC)mat cells and the single X chromosome in the 45,X cells are derived from a common X chromosome of maternal origin, with no paternally derived sex chromosome. It is likely, therefore, that a parthenogenetic activation took place around the time of fertilisation of a sperm missing a sex chromosome, resulting in the generation of the 46,XX cell lineage with upid (AC)mat by endoreplication (the replication of DNA without the subsequent completion of mitosis) of one blastomere containing a female pronucleus and the 45,X cell lineage with biparentally derived autosomes and a maternally derived X chromosome by union of male and female pronuclei (figure 2), although it is also possible that a paternally derived sex chromosome was present in the sperm but was lost from the normal

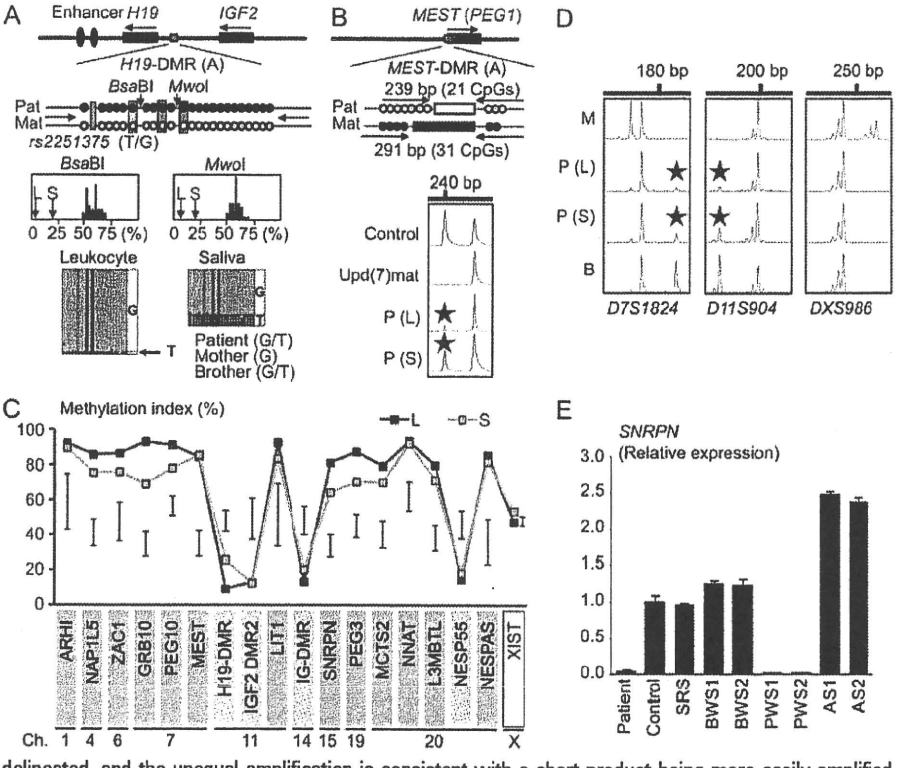

Figure 1 Representative molecular results. Pat, paternally derived allele; Mat, maternally derived allele; P, patient; M, mother; B, brother; L, leukocytes; and S, saliva cells. Filled and open circles in A and B represent methylated and unmethylated cytosine residues at the CpG dinucleotides, respectively. A. Methylation patterns of the *H19*-DMR (A) harbouring 23 CpG dinucleotides and the T/G SNP (*rs2251375*) (a grey box). The PCR products are digested with *Bsa*BI when the cytosine at the sixth CpG dinucleotide (highlighted in yellow) is methylated and with *Mwo*I when the two cytosines at the ninth and the 11th CpG dinucleotides (highlighted in orange) are methylated. For the bio-COBRA data, the black histograms represent the distribution of methylation indices (%) in 50 control participants, and L and S denote the methylation indices for leukocytes and saliva cells of this patient, respectively. For the bisulfite sequencing data, each line indicates a single clone. B. Methylated and unmethylated allele-specific PCR analysis for the *MEST*-DMR (A). In a control participant, the PCR products for methylated and unmethylated alleles are delineated, and the unequal amplification is consistent with a short product being more easily amplified than a long product. In a previously reported patient with upd(7)mat,[8] the methylated allele only is amplified. In this patient, major peaks for the methylated allele and minor peaks for the unmethylated allele (red asterisks) are detected. C. Methylation patterns for the 18 DMRs examined. The DMRs highlighted in blue and pink are methylated after paternal and maternal transmissions, respectively. The black vertical bars indicate the reference data (maximum–minimum) in 20 normal control participants, using leukocyte genomic DNA (for the *XIST*-DMR, 16 female data are shown). D. Representative microsatellite analysis. Minor peaks (red asterisks) have been identified for *D7S1824* and *D11S904* but not for *DXS986* of the patient. Since the peaks for *D7S1824* and *D11S904* are absent in the mother and clearly present in the brother, they are assessed to be of paternal origin. E. Relative expression level (mean ± SD) of *SNRPN* on chromosome 15. The data have been normalised against *TBP*. SRS, an SRS patient with an epimutation (hypomethylation) of the *H19*-DMR; BWS1, a BWS patient with an epimutation (hypermethylation) of the *H19*-DMR; BWS2, a BWS patient with upd(11)pat; PWS1, a PWS patient with upd(15)mat; PWS2, a PWS patient with an epimutation (hypermethylation) of the *SNRPN*-DMR; AS1, an Angelman syndrome (AS) patient with upd(15)pat; and AS2, an AS patient with an epimutation (hypomethylation) of the *SNRPN*-DMR.

cell lineage at the very early developmental stage. Hence, in a strict sense, this patient is neither a chimera resulting from the fusion of two different zygotes nor a mosaic caused by a mitotic error of a single zygote. In this regard, a triploid cell stage is assumed in the generation of a upid(AC)mat cell lineage, and such triploid cells may have been detected in skin fibroblasts of the patient reported by Horike *et al*.[3]

The upid(AC)mat cells accounted for the majority of leukocytes even in adulthood of this patient, despite global negative selective pressure.[12 13] This phenomenon, though intriguing, would not be unexpected in human studies because leukocytes are usually utilised for genetic analyses. Rather, if the upid(AC)mat cells were barely present in leukocytes, they would not have been detected. It is likely, therefore, that upid(AC)mat cells have occupied a relatively large portion of the definitive haematopoietic tissues primarily as a stochastic event. Furthermore, parthenogenetic chimera mouse studies have revealed that parthenogenetic cells are found at a relatively high frequency in some tissues/organs including blood and are barely identified in other tissues/organs such as skeletal muscle and liver.[13] Such a possible tissue-specific selection in favour of the preservation of parthenogenetic cells in the definitive haematopoietic tissues may also be relevant to the predominance of the upid(AC)mat cells in leukocytes. In addition, a reduced growth potential of 45,X cells[14] may also have contributed to the skewed ratio of the two cell lineages.

Clinical features of this patient would be determined by several factors. They include: (1) the ratio of two cell lineages in various tissues/organs, (2) the number of imprinted regions or DMRs relevant to the development of specific imprinting disorders (eg, plural regions/DMRs on chromosomes 7 and 11 for SRS[9 10] and a single region/DMR on chromosome 15 for Prader–Willi syndrome (PWS)),[15] (3) the degree of clinical effects of dysregulated imprinted regions/DMRs (an (epi)dominant effect has been

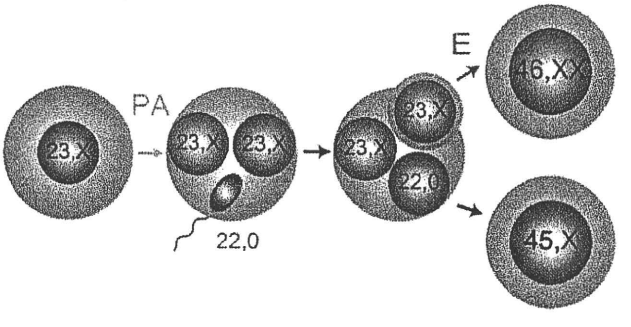

Figure 2 Schematic representation of the generation of the upid(AC)mat 46,XX cell lineage and the non-upd 45,X cell lineage. Polar bodies are not shown. PA, parthenogenetic activation; and E, endoreplication of one blastomere containing a female pronucleus.

assumed for the 11p15.5 imprinted regions including the *IGF2–H19* domain on the basis of SRS or Beckwith–Wiedemann syndrome (BWS) phenotype in patients with multilocus hypomethylation[16] and BWS-like phenotype in patients with a upid (AC)pat cell lineage,[17] a mirror image of a upid(AC)mat cell lineage), (4) expression levels of imprinted genes in upid(AC)mat cells (although *SNRPN* expression of this patient was consistent with upid(AC)mat cells being predominant in leukocytes, complicated expression patterns have been identified for several imprinted genes in androgenetic and parthenogenetic fetal mice, probably because of perturbed *cis*- and *trans*-acting regulatory mechanisms)[18] and (5) unmasking of possible maternally inherited recessive mutation(s) in upid(AC)mat cells.[19] Collectively, it appears that the extent of overall (epi)genetic aberrations exceeded the threshold level for the development of SRS phenotype and horseshoe kidney characteristic of TS[4] but remained below the threshold level for the occurrence of other imprinting disorders or recessive Mendelian disorders.

In summary, we identified a upid(AC)mat 46,XX cell lineage in a woman with an SRS-like phenotype and a 45,X cell lineage accompanied by autosomal haploid sets of biparental origin. This report will facilitate further identification of patients with a upid(AC)mat cell lineage and better clarification of the clinical phenotypes in such patients.

Acknowledgements We thank the patient and her family members for their participation in this study. We also thank Dr. Toshiro Nagai for providing us with blood samples of patients with Prader–Willi syndrome.

Funding This work was supported by grants from the Ministry of Health, Labor, and Welfare and from the Ministry of Education, Science, Sports and Culture.

Competing interests None.

Patient consent Obtained.

Ethics approval This study was conducted with the approval of the Institutional Review Board Committees at National Center for Child health and Development.

Contributors Drs Kazuki Yamazawa (first author) and Kazuhiko Nakabayashi (second author) contributed equally to this work.

Provenance and peer review Not commissioned; externally peer reviewed.

REFERENCES

1. **McGrath J,** Solter D. Completion of mouse embryogenesis requires both the maternal and paternal genomes. *Cell* 1984;**37**:179–83.
2. **Strain L,** Warner JP, Johnston T, Bonthron DT. A human parthenogenetic chimaera. *Nat Genet* 1995;**11**:164–9.
3. **Horike S,** Ferreira JC, Meguro-Horike M, Choufani S, Smith AC, Shuman C, Meschino W, Chitayat D, Zackai E, Scherer SW, Weksberg R. Screening of DNA methylation at the H19 promoter or the distal region of its ICR1 ensures efficient detection of chromosome 11p15 epimutations in Russell–Silver syndrome. *Am J Med Genet Part A* 2009;**149A**:2415–23.
4. **Styne D,** Grumbach M. Puberty: ontogeny, neuroendocrinology, physiology, and disorders. In: Kronenberg H, Melmed M, Polonsky K, Larsen P, eds. *Williams textbook of endocrinology*, 11th edn. Philadelphia: Saunders 2008:969–1166.
5. **Thiede C,** Prange-Krex G, Freiberg-Richter J, Bornhauser M, Ehninger G. Buccal swabs but not mouthwash samples can be used to obtain pretransplant DNA fingerprints from recipients of allogeneic bone marrow transplants. *Bone Marrow Transplant* 2000;**25**:575–7.
6. **Brena RM,** Auer H, Kornacker K, Hackanson B, Raval A, Byrd JC, Plass C. Accurate quantification of DNA methylation using combined bisulfite restriction analysis coupled with the Agilent 2100 Bioanalyzer platform. *Nucleic Acids Res* 2006;**34**:e17.
7. **Yamazawa K,** Kagami M, Nagai T, Kondoh T, Onigata K, Maeyama K, Hasegawa T, Hasegawa Y, Yamazaki T, Mizuno S, Miyoshi Y, Miyagawa S, Horikawa R, Matsuoka K, Ogata T. Molecular and clinical findings and their correlations in Silver–Russell syndrome: implications for a positive role of IGF2 in growth determination and differential imprinting regulation of the IGF2-H19 domain in bodies and placentas. *J Mol Med* 2008;**86**:1171–81.
8. **Yamazawa K,** Kagami M, Ogawa M, Horikawa R, Ogata T. Placental hypoplasia in maternal uniparental disomy for chromosome 7. *Am J Med Genet Part A* 2008;**146A**:514–16.
9. **Abu-Amero S,** Monk D, Frost J, Preece M, Stanier P, Moore GE. The genetic aetiology of Silver–Russell syndrome. *J Med Genet* 2008;**45**:193–9.
10. **Eggermann T,** Eggermann K, Schonherr N. Growth retardation versus overgrowth: Silver–Russell syndrome is genetically opposite to Beckwith–Wiedemann syndrome. *Trends Genet* 2008;**24**:195–204.
11. **Goto T,** Monk M. Regulation of X-chromosome inactivation in development in mice and humans. *Microbiol Mol Biol Rev* 1998;**62**:362–78.
12. **Nagy A,** Sass M, Markkula M. Systematic non-uniform distribution of parthenogenetic cells in adult mouse chimaeras. *Development* 1989;**106**:321–4.
13. **Fundele R,** Norris ML, Barton SC, Reik W, Surani MA. Systematic elimination of parthenogenetic cells in mouse chimeras. *Development* 1989;**106**:29–35.
14. **Verp MS,** Rosinsky B, Le Beau MM, Martin AO, Kaplan R, Wallemark CB, Otano L, Simpson JL. Growth disadvantage of 45, X and 46, X, del(X)(p11) fibroblasts. *Clin Genet* 1988;**33**:277–85.
15. **Horsthemke B,** Wagstaff J. Mechanisms of imprinting of the Prader–Willi/Angelman region. *Am J Med Genet A* 2008;**146A**:2041–52.
16. **Azzi S,** Rossignol S, Steunou V, Sas T, Thibaud N, Danton F, Le Jule M, Heinrichs C, Cabrol S, Gicquel C, Le Bouc Y, Netchine I. Multilocus methylation analysis in a large cohort of 11p15-related foetal growth disorders (Russell Silver and Beckwith Wiedemann syndromes) reveals simultaneous loss of methylation at paternal and maternal imprinted loci. *Hum Mol Genet* 2009;**18**:4724–33.
17. **Wilson M,** Peters G, Bennetts B, McGillivray G, Wu ZH, Poon C, Algar E. The clinical phenotype of mosaicism for genome-wide paternal uniparental disomy: two new reports. *Am J Med Genet Part A* 2008;**146A**:137–48.
18. **Ogawa H,** Wu Q, Komiyama J, Obata Y, Kono T. Disruption of parental-specific expression of imprinted genes in uniparental fetuses. *FEBS Lett* 2006;**580**:5377–84.
19. **Engel E.** A fascination with chromosome rescue in uniparental disomy: Mendelian recessive outlaws and imprinting copyrights infringements. *Eur J Hum Genet* 2006;**14**:1158–69.